

# Highly Linearized Twisted Iridium(III) complexes

Ross Davidson,<sup>†\*</sup> Yu-Ting Hsu,<sup>†</sup> Gareth C. Griffiths,<sup>‡</sup> Chenfei Li,<sup>†¶</sup> Dmitry Yufit<sup>†</sup>, Robert  
Pal,<sup>†</sup> Andrew Beeby<sup>†\*</sup>

<sup>†</sup>*Department of Chemistry, University of Durham, South Road, Durham, DH1 3LE, England,  
UK*

<sup>‡</sup>*Department of Physics, University of Durham, South Road, Durham, DH1 3LE, England,  
UK*

<sup>¶</sup>*School of Chemistry, University of St Andrews, St Andrews, KY16 9AJ, Scotland,  
UK*

---

**ABSTRACT:** Improving the spatial alignment of emitting molecules has long been a goal of organic- light-emitting-diode development to improve device efficiencies and to generate polarized emission. Herein we describe a simple approach employing Sonogashira coupling with alkyne iridium(phenylpyridine)<sub>2</sub>(acetylacetonate) synthons (**2-5**) to generate eight linear iridium complexes (**6-13**) with crystallographically determined lengths of up to 5 nm. By embedding these ‘long’ complexes into a polymer matrix and stretching it an improvement of polarization ratio of an unstretched and stretched film up to 7.1 times was achieved. Additionally, through the inclusion of ‘twists’ in the complexes the electronic coupling between the iridium center and substituent was controlled giving a system where the emission behavior is independent of the length.

**KEYWORDS:** Iridium, polarization, OLED, mechanical alignment

---

## INTRODUCTION

The incorporation of phosphorescent emitters into OLEDs has been one of the most significant developments in the area of display technology due to the potential to harvest both singlet and triplet excitons, giving them a theoretical maximum internal quantum efficiency of 100 %.<sup>1</sup> However, in practice the external quantum efficiencies often fall short of this. One of the causes for this is the orientation of the emitter: in a typical solution processed OLED the molecules are randomly orientated, this results in photons trapped in the film structure, lost to surface plasmons and wave guide modes, ultimately reduces the external quantum efficiency (EQE) of the device. A possible solution to this is to align the emitting molecules, controlling the direction and orientation of the photons being emitted i.e. polarizing the emission.<sup>2-8</sup> This would not only improve the EQE but also generate plane polarized light allowing for a greater range of applications such as 3D projection, holography, and adaptive

phase and amplitude modulation SLM. In order to align the emissions transition dipoles the emitting molecule needs to have: i) a single transition dipole moment in a single specific direction, iridium complexes, specifically  $\text{Ir}(2\text{-phenylpyridine})_2(\text{L}\cap\text{L})$  (where  $\text{L}\cap\text{L}$  can be a range of ancillary ligands) have a strong transition dipole moment parallel to the  $\text{N}_{\text{ppy}}\text{-Ir-N}_{\text{ppy}}$  axis;<sup>2</sup> and ii) the molecule must have a preferred orientation with respect to the substrate. Orientating the molecules with respect to the substrate can be achieved in a number of ways, by deposition as Langmuir-Blodgett films, rubbing or shearing, mechanical stretching, prealigned substrates, epitaxial vapor deposition, and fractional transfer on aligned substituents. Recently, Thompson, Moon and Mayr have demonstrated that it is possible to horizontally align emissive complexes ( $\text{Ir}(2\text{-phenylpyridine})_2(\text{acetylacetonate})$  or  $\text{Ir}(2\text{-phenylpyridine})_3$ , etc.) through the choice of host molecules ( $\text{N,N}'\text{-dicarbazolyl-4,4'}$ biphenyl [CBP] or bis-4,6-(3,5-di-3-pyridylphenyl)-2-methylpyrimidine [B3PYMPM]) to achieve horizontal:vertical ratios as high as 75:25, this was attributed both to the high aspect ratio of the CBP and B3PYMPM and a proposed supramolecular interaction between the host molecule and the iridium complexes due to  $\pi\text{-}\pi$  interactions which effectively increased the aspect ratio of the complex.<sup>3, 7-10</sup> The iridium complexes used in these studies have aspect ratios of *ca.* 1 and as a result the orientations of these molecules were entirely governed by interactions with the host molecules, greatly restricting the choice of host materials that could be used in devices. A possible solution to this is to greatly increase the aspect ratio of the emitting molecules, allowing alignment by other processes. A linear iridium complex it needs to be a heteroleptic complex with 2-phenylpyridine (ppy) and an ancillary ligand, e.g. acetylacetonate (acac) or picolinate (pic), and any extensions be made at the 4-position of the ppy pyridine. Two examples of this type of modification have been reported  $\text{Ir}(2,4\text{-diphenylpyridine})_2(\text{acac})$  ( $\text{Ir}(\text{Phppy})_2(\text{acac})$ ,  $\lambda_{\text{emis}} = 560 \text{ nm}$ ) and  $\text{Ir}(2\text{-phenyl-4-(phenylethynyl)pyridine})_2(\text{acac})$  ( $\text{Ir}(\text{Ph}\equiv\text{ppy})_2(\text{acac})$ ,  $\lambda_{\text{emis}} = 570 \text{ nm}$ ),<sup>11, 12</sup> with aspect ratios

of 1.97 and 2.54 respectively, however, in both cases the emissions of the complexes were significantly redshifted relative to that of the parent complex Ir(ppy)<sub>2</sub>(acac) ( $\lambda_{\text{emis}} = 520 \text{ nm}$ ) due to the increased conjugation of the substituent on the pyridine ring as a molecules length increased, additionally with the increased flexibility of the molecules facilitating non-radiative decay processes the photo luminescent quantum yields ( $\Phi_{\text{PL}}$ ) decreased. Therefore, any substituent used to extend the aspect ratio of the molecules also needs to be electronically decoupled from the emissive center such that the photophysical properties of the core 'Ir(ppy)<sub>2</sub>L' remains intact. Kozhevnikov and co-workers. has demonstrated that the decoupling can be achieved by adding a twist between the ppy ligand and the substituent, achieved by replacing the 4-phenyl group with a mesityl. The steric hindrance of the two ortho-methyl groups resulted in a twist of the molecule effectively decoupling and prevented red shifting of the emission, in fact a significant enhancement of  $\Phi_{\text{PL}}$  and increased solubility was observed.<sup>13</sup> Therefore in this investigation we seek to improve the horizontal alignment of iridium based complexes by increasing the aspect ratio while maintaining the photophysical behavior of the parent compound by the inclusion of 'twists' that decouple the electronic properties of the substituents from the core complex. Ir(ppy)<sub>2</sub>(acac) based complexes were chosen to for the proof of concept because of their ease of synthesis and well established physical properties and a transition dipole moment perpendicular to the axis being lengthened.

## Experimental section

### Synthesis

**General details.** NMR spectra were recorded in deuterated solvent solutions on a Varian VNMRs-600 spectrometer and referenced against solvent resonances (<sup>1</sup>H, <sup>13</sup>C). ESMS data were recorded on a TQD mass spectrometer (Waters Ltd, UK) in either

acetonitrile or methanol, GCMS data were recorded on Trace GCMS (ThermoFinnigan) GCMS recorded in DCM, ASAP data were recorded on a Xevo QTOF (Waters) high resolution, accurate mass tandem mass spectrometer equipped with Atmospheric Pressure Gas Chromatography (APGC) and Atmospheric Solids Analysis Probe (ASAP). MALDI data were recorded on a Bruker Autoflex II ToF/FoF spectrometer. Microanalyses were performed by Elemental Analysis Service, London Metropolitan University, UK or Elemental Microanalysis service, Durham University, UK.

*4-(4-((triisopropylsilyl)ethynyl)phenyl)pyridine*. THF (dry, 50 mL) and Et<sub>3</sub>N (15 mL) were added to 4-(4-bromophenyl)pyridine (5.0 g, 21.5 mmol), Pd(PPh<sub>3</sub>)<sub>2</sub>Cl<sub>2</sub> (1.1 g, 1.6 mmol) and CuI (285 mg, 1.5 mmol). The solution was degassed by three freeze-pump-thaw cycles before triisopropylsilyl acetylene (5.60 mL, 4.55 g, 25 mmol) was added. The solution was heated to reflux for 16 hours before the solvent was removed. The product was purified via column chromatography on silica gel eluted with a solvent gradient from neat DCM to neat Et<sub>2</sub>O. The oil was dissolved in Et<sub>2</sub>O before etheryl hydrogen chloride was added, immediately forming a precipitate. This was continued until no additional precipitate formed. At this stage, the precipitate was collected by filtration. The white powder was dissolved in DCM and washed with an ammonium hydroxide solution. The organic layer was collected, dried over MgSO<sub>4</sub> and the solvent removed, to give a colourless oil. Yield: 6.35 g (88 %). **<sup>1</sup>H NMR** (700 MHz; CDCl<sub>3</sub>): δ<sub>H</sub> 8.65 (d,  $J^3_{\text{HH}} = 6.0$  Hz, 2H, H<sub>a</sub>), 7.58-7.55 (m, 4H, H<sub>c</sub>+H<sub>d</sub>), 7.47 (d,  $J^3_{\text{HH}} = 6.0$  Hz, 2H, H<sub>b</sub>), 1.13 (pseudo singlet, 21H, H<sub>e</sub>+H<sub>f</sub>) ppm. **<sup>13</sup>C{<sup>1</sup>H} NMR** (176 MHz; CDCl<sub>3</sub>): δ<sub>C</sub> 150.2, 147.4, 137.7, 132.7, 126.7, 124.3, 121.3, 106.3, 92.6, 18.6, 11.2 ppm. **ES-MS**: m/z 336.060 [M+H]<sup>+</sup>. **Anal. Calc.** for C<sub>22</sub>H<sub>29</sub>NSi: C, 78.75; H, 8.71; N, 4.17 %. **Found**: C, 78.68; H, 8.82; N, 4.26 %.

*4-(2-methyl-4-((triisopropylsilyl)ethynyl)phenyl)pyridine*. The same procedure as for 4-(4-((triisopropylsilyl)ethynyl)phenyl)pyridine, except 4-(4-bromo-2-methylphenyl)pyridine was used in place of 4-(4-bromophenyl)pyridine to give a colourless oil. Yield: 6.77 g (90 %). **<sup>1</sup>H NMR** (700 MHz; CDCl<sub>3</sub>): δ<sub>H</sub> 8.63 (d,  $J^3_{\text{HH}} = 6.0$  Hz, 2H, H<sub>a</sub>), 7.40 (d,  $J^4_{\text{HH}} = 1.6$  Hz, 1H, H<sub>e</sub>), 7.36 (dd,  $J^3_{\text{HH}} = 7.7$  Hz,  $J^4_{\text{HH}} = 1.6$  Hz, 1H, H<sub>d</sub>), 7.20 (d,  $J^3_{\text{HH}} = 6.0$  Hz, 2H, H<sub>b</sub>), 7.12 (d,  $J^3_{\text{HH}} = 7.8$  Hz, 1H, H<sub>c</sub>), 2.24 (s, 3H, H<sub>f</sub>), 1.13 (pseudo singlet, 21H, H<sub>g</sub>+H<sub>h</sub>) ppm. **<sup>13</sup>C{<sup>1</sup>H} NMR** (176 MHz; CDCl<sub>3</sub>): δ<sub>C</sub> 149.6, 149.0, 139.0, 135.0, 134.0, 129.6, 129.1, 123.9, 123.6, 106.5, 91.3, 20.0, 18.6, 11.3 ppm. **ES-MS**: m/z 350.865 [M+H]<sup>+</sup>. **Anal. Calc.** for C<sub>23</sub>H<sub>31</sub>NSi: C, 79.02; H, 8.94; N, 4.01 %. **Found**: C, 79.16; H, 9.02; N, 4.15 %.

*4-(2,3,5,6-tetramethyl-4-((triisopropylsilyl)ethynyl)phenyl)pyridine*. The same procedure as for 4-(4-((triisopropylsilyl)ethynyl)phenyl)pyridine, except 4-(4-iodo-2,3,5,6-tetramethylphenyl)pyridine was used in place of 4-(4-bromophenyl)pyridine to give a colourless oil. Yield: 6.32 g (75 %). **<sup>1</sup>H NMR** (700 MHz; CDCl<sub>3</sub>): δ<sub>H</sub> 8.67 (d,  $J^3_{\text{HH}} = 5.0$  Hz, 2H, H<sub>a</sub>), 7.05 (d,  $J^3_{\text{HH}} = 5.9$  Hz, 2H, H<sub>b</sub>), 2.48 (s, 6H, H<sub>c</sub>), 1.88 (s, 6H, H<sub>d</sub>), 1.15 (pseudo singlet, 21H, H<sub>e</sub>+H<sub>f</sub>) ppm. **<sup>13</sup>C{<sup>1</sup>H} NMR** (176 MHz; CDCl<sub>3</sub>): δ<sub>C</sub> 150.7, 149.8, 139.2, 136.61, 130.8, 124.6, 123.8, 105.3, 99.0, 18.7, 18.5, 17.8, 11.3 ppm. **ES-MS**: m/z 392.278 [M+H]<sup>+</sup>. **Anal. Calc.** for C<sub>26</sub>H<sub>37</sub>NSi: C, 79.73; H, 9.52; N, 3.58 %. **Found**: C, 79.67; H, 9.50; N, 3.52 %.

*2-phenyl-4-(2,3,5,6-tetramethylphenyl)pyridine (L<sup>1</sup>H)*. 4-(2,3,5,6-tetramethylphenyl)pyridine (5.0 g, 23.6 mmol) was dissolved in THF (100 mL) before the solution was cooled to -78 °C. Phenyllithium (1.9 M, 49.6 mL, 94.4 mmol) was added to the

solution slowly. The temperature was maintained at  $-78\text{ }^{\circ}\text{C}$  for 1 hour before being allowed to warm to room temperature. Stirring was continued for an additional 6 hours before the reaction was quenched by pouring the solution into water. The solution was extracted with DCM, dried over  $\text{MgSO}_4$  and the solvent removed. The product was purified by silica chromatography eluted with a solvent gradient from neat hexane to neat DCM, yielding a yellow oil. Yield: 2.85 g (42 %).  **$^1\text{H}$  NMR** (700 MHz;  $\text{CDCl}_3$ ):  $\delta_{\text{H}}$  8.74 (dd,  $J^3_{\text{HH}} = 4.9\text{ Hz}$ ,  $J^4_{\text{HH}} = 0.9\text{ Hz}$ , 1H,  $\text{H}_a$ ), 8.03 (d,  $J^3_{\text{HH}} = 8.0\text{ Hz}$ , 2H,  $\text{H}_d$ ), 7.55 (s, 1H,  $\text{H}_c$ ), 7.49-7.46 (m, 2H,  $\text{H}_e$ ), 7.43-7.40 (m, 1H,  $\text{H}_f$ ), 7.04-7.03 (m, 2H,  $\text{H}_b+\text{H}_j$ ), 2.28 (s, 6H,  $\text{H}_g$ ), 1.92 (s, 6H,  $\text{H}_h$ ) ppm.  **$^{13}\text{C}\{^1\text{H}\}$  NMR** (176 MHz;  $\text{CDCl}_3$ ):  $\delta_{\text{C}}$  157.4, 151.6, 149.7, 139.5, 139.2, 133.9, 131.1, 129.0, 128.7, 126.9, 123.2, 121.5, 20.0, 17.1 ppm. **ES-MS**:  $m/z$  288.174  $[\text{M}+\text{H}]^+$ . **Anal. Calc.** for  $\text{C}_{21}\text{H}_{21}\text{N}$ : C, 87.76; H, 7.37; N, 4.87 %. **Found**: C, 87.60; H, 7.49; N, 4.87 %.

*2-phenyl-4-((triisopropylsilyl)ethynyl)pyridine (L<sup>2</sup>H)*. The same procedure as for **L<sup>1</sup>H**, except 4-((triisopropylsilyl)ethynyl)pyridine was used in place of 4-(2,3,5,6-tetramethylphenyl)pyridine to give a yellow oil. Yield: 2.06 g (40 %).  **$^1\text{H}$  NMR** (700 MHz;  $\text{CDCl}_3$ ):  $\delta_{\text{H}}$  8.64 (dd,  $J^3_{\text{HH}} = 5.1\text{ Hz}$ ,  $J^4_{\text{HH}} = 1.9\text{ Hz}$ , 1H,  $\text{H}_a$ ), 7.98 (d,  $J^3_{\text{HH}} = 8.0\text{ Hz}$ , 2H,  $\text{H}_d$ ), 7.75 (s, 1H,  $\text{H}_c$ ), 7.48-7.45 (m, 2H,  $\text{H}_e$ ), 7.42-7.40 (m, 1H,  $\text{H}_f$ ), 7.26 (d,  $J^3_{\text{HH}} = 6.4\text{ Hz}$ , 1H,  $\text{H}_b$ ), 1.15 (pseudo singlet, 21H,  $\text{H}_g+\text{H}_h$ ) ppm.  **$^{13}\text{C}\{^1\text{H}\}$  NMR** (176 MHz;  $\text{CDCl}_3$ ):  $\delta_{\text{C}}$  157.8, 149.8, 139.0, 132.4, 129.5, 129.0, 127.2, 124.5, 123.1, 104.6, 96.6, 18.9, 11.4 ppm. **ES-MS**:  $m/z$  336.214  $[\text{M}+\text{H}]^+$ . **Anal. Calc.** for  $\text{C}_{22}\text{H}_{29}\text{NSi}$ : C, 78.75; H, 8.71; N, 4.17 %. **Found**: C, 78.60; H, 8.83; N, 4.25 %.

*2-phenyl-4-(4-((triisopropylsilyl)ethynyl)phenyl)pyridine (L<sup>3</sup>H)*. The same procedure as for **L<sup>1</sup>H**, except 4-(4-((triisopropylsilyl)ethynyl)phenyl)pyridine was used in place of 4-

(2,3,5,6-tetramethylphenyl)pyridine to give a yellow oil. Yield: 3.48 g (55 %). **<sup>1</sup>H NMR** (700 MHz; CDCl<sub>3</sub>): δ<sub>H</sub> 8.73 (d,  $J^3_{\text{HH}} = 5.1$  Hz, 1H, H<sub>a</sub>), 8.05 (d,  $J^3_{\text{HH}} = 8.0$  Hz, 2H, H<sub>d</sub>), 7.89 (s, 1H, H<sub>c</sub>), 7.64-7.60 (m, 4H, H<sub>g</sub>+H<sub>h</sub>), 7.51-7.49 (m, 2H, H<sub>e</sub>), 7.45-7.43 (m, 1H, H<sub>f</sub>), 7.40 (dd,  $J^3_{\text{HH}} = 5.1$  Hz,  $J^4_{\text{HH}} = 1.7$  Hz, 1H, H<sub>b</sub>), 1.18 (pseudo singlet, 21H, H<sub>i</sub>+H<sub>j</sub>) ppm. **<sup>13</sup>C{<sup>1</sup>H} NMR** (176 MHz; CDCl<sub>3</sub>): δ<sub>C</sub> 158.2, 150.1, 148.3, 139.3, 138.1, 132.7, 129.0, 128.7, 127.0, 126.8, 124.3, 119.9, 118.4, 106.4, 92.6, 18.7, 11.3 ppm. **MS-ASAP**: m/z 412.219 [M+H]<sup>+</sup>. **Anal. Calc.** for C<sub>28</sub>H<sub>33</sub>NSi: C, 81.69; H, 8.08; N, 3.40 %. **Found**: C, 81.75; H, 8.17; N, 3.44 %.

*4-(2-methyl-4-((triisopropylsilyl)ethynyl)phenyl)-2-phenylpyridine (L<sup>4</sup>H)*. The same procedure as for **L<sup>1</sup>H**, except 4-(2-methyl-4-((triisopropylsilyl)ethynyl)phenyl)pyridine was used in place of 4-(2,3,5,6-tetramethylphenyl)pyridine to give a yellow oil. Yield: 3.14 g (48 %). **<sup>1</sup>H NMR** (700 MHz; CDCl<sub>3</sub>): δ<sub>H</sub> 8.72 (dd,  $J^3_{\text{HH}} = 5.1$  Hz,  $J^4_{\text{HH}} = 0.8$  Hz, 1H, H<sub>a</sub>), 8.01 (dd,  $J^3_{\text{HH}} = 7.0$  Hz, 2H, H<sub>d</sub>), 7.66 (s, 1H, H<sub>c</sub>), 7.51-7.48 (m, 2H, H<sub>e</sub>), 7.45-7.41 (m, 3H, H<sub>f</sub>+H<sub>h</sub>+H<sub>i</sub>), 7.21 (d,  $J^3_{\text{HH}} = 7.8$  Hz, 1H, H<sub>g</sub>), 7.17 (dd,  $J^3_{\text{HH}} = 5.0$  Hz,  $J^4_{\text{HH}} = 1.6$  Hz, 1H, H<sub>b</sub>), 2.30 (s, 3H, H<sub>j</sub>), 1.16 (pseudo singlet, 21H, H<sub>k</sub>+H<sub>l</sub>) ppm. **<sup>13</sup>C{<sup>1</sup>H} NMR** (176 MHz; CDCl<sub>3</sub>): δ<sub>C</sub> 157.2, 149.9, 149.5, 139.3, 139.2, 135.1, 134.0, 129.7, 129.1, 129.0, 128.7, 126.9, 123.6, 122.4, 120.9, 106.6, 91.3, 20.1, 18.6, 11.3 ppm. **ES-MS**: m/z 426.243 [M+H]<sup>+</sup>. **Anal. Calc.** for C<sub>29</sub>H<sub>35</sub>NSi: C, 81.82; H, 8.29; N, 3.29 %. **Found**: C, 81.90; H, 8.35; N, 3.46 %.

*2-phenyl-4-(2,3,5,6-tetramethyl-4-((triisopropylsilyl)ethynyl)phenyl)pyridine (L<sup>5</sup>H)*. The same procedure as for **L<sup>1</sup>H**, except 4-(2,3,5,6-tetramethyl-4-((triisopropylsilyl)ethynyl)phenyl)pyridine was used in place of 4-(2,3,5,6-tetramethylphenyl)pyridine to give a yellow oil. Yield: 4.50 g (41 %). **<sup>1</sup>H NMR** (700 MHz; CDCl<sub>3</sub>): δ<sub>H</sub> 8.75 (d,  $J^3_{\text{HH}} = 4.9$  Hz,  $J^4_{\text{HH}} = 0.9$  Hz, 1H, H<sub>a</sub>), 8.02 (dd,  $J^3_{\text{HH}} = 7.0$  Hz,  $J^4_{\text{HH}} = 1.2$

Hz, 2H, H<sub>d</sub>), 7.50 (s, 1H, H<sub>c</sub>), 7.49-7.46 (m, 2H, H<sub>e</sub>), 7.43-7.40 (m, 1H, H<sub>f</sub>), 7.00 (dd  $J^3_{\text{HH}} = 4.9$  Hz,  $J^4_{\text{HH}} = 1.5$  Hz, 1H, H<sub>b</sub>), 2.49 (s, 6H, H<sub>g</sub>), 1.93 (s, 6H, H<sub>h</sub>), 1.16 (pseudo singlet, 21H, H<sub>i</sub>+H<sub>j</sub>) ppm.  $^{13}\text{C}\{^1\text{H}\}$  NMR (176 MHz; CDCl<sub>3</sub>):  $\delta_{\text{C}}$  157.5, 151.5, 149.7, 139.5, 139.0, 136.6, 130.9, 129.1, 128.7, 126.9, 123.8, 123.0, 121.2, 105.3, 99.0, 18.7, 18.5, 17.8, 11.3 ppm. **MS-ASAP:** m/z 468.308 [M+H]<sup>+</sup>. **Anal. Calc.** for C<sub>32</sub>H<sub>41</sub>NSi: C, 82.17; H, 8.84; N, 2.99 %. **Found:** C, 81.99; H, 8.93; N, 3.22 %.

**Iridium coordination general procedure.** IrCl<sub>3</sub>·3H<sub>2</sub>O (408 mg, 1.1 mmol) was added to a solution containing L<sup>1</sup>H – L<sup>5</sup>H (3.48 mmol), ethoxyethanol (30 mL) and water (15 mL). The solution was heated to 110 °C for 12 hours before being cooled and poured into water (300 mL), forming a precipitate. The precipitate was dissolved in DCM and dried over MgSO<sub>4</sub> before being passed through a silica plug. The residue was dissolved in ethoxyethanol (30 mL), acetylacetone (5 mL) and K<sub>2</sub>CO<sub>3</sub> (276 mg, 2.0 mmol) were added and the solution heated to 90 °C for 12 hours. The solution was cooled and poured into water (300 mL), forming a precipitate that was collected via filtration. The precipitate was dissolved in DCM and dried over MgSO<sub>4</sub> before the product was purified via silica chromatography eluted by DCM, collecting the emissive band.

*Ir(L<sup>1</sup>)<sub>2</sub>(acac) (1)*. A bright green solid. Crystals were grown by evaporation of a DCM/hexane solution. Yield: 589 mg (62 %).  $^1\text{H}$  NMR (700 MHz; CD<sub>2</sub>Cl<sub>2</sub>):  $\delta_{\text{H}}$  8.59 (dd  $J^3_{\text{HH}} = 5.7$  Hz, 2H, H<sub>a</sub>), 7.69 (d,  $J^4_{\text{HH}} = 2.0$  Hz, 2H, H<sub>c</sub>), 7.55 (dd,  $J^3_{\text{HH}} = 7.8$  Hz,  $J^4_{\text{HH}} = 1.7$  Hz, 2H, H<sub>g</sub>), 7.09 (s, 2H, H<sub>h</sub>), 7.03 (dd,  $J^3_{\text{HH}} = 5.8$  Hz,  $J^4_{\text{HH}} = 1.8$  Hz, 2H, H<sub>b</sub>), 6.86 (td,  $J^3_{\text{HH}} = 7.4$  Hz,  $J^4_{\text{HH}} = 1.7$  Hz, 2H, H<sub>f</sub>), 6.76 (td,  $J^3_{\text{HH}} = 7.4$  Hz,  $J^4_{\text{HH}} = 1.7$  Hz, 2H, H<sub>e</sub>), 6.41 (dd,  $J^3_{\text{HH}} = 7.8$  Hz,  $J^4_{\text{HH}} = 1.6$  Hz, 2H, H<sub>d</sub>), 5.38 (s, 1H, H<sub>m</sub>), 2.33-2.32 (m, 12H, H<sub>i</sub>+H<sub>j</sub>), 2.09 (s,

6H, H<sub>l</sub> or H<sub>k</sub>), 2.02 (s, 6H, H<sub>l</sub> or H<sub>k</sub>), 1.88 (s, 6H, H<sub>n</sub>) ppm. **<sup>13</sup>C{<sup>1</sup>H} NMR** (176 MHz; CD<sub>2</sub>Cl<sub>2</sub>): δ<sub>C</sub> 184.7, 168.1, 152.3, 147.9, 147.4, 145.3, 138.9, 133.9, 133.0, 131.2, 131.1, 128.7, 123.8, 123.2, 120.7, 119.8, 100.4, 28.3, 19.8, 16.9 ppm. **MS-MALDI**: m/z 864.4 [M]<sup>+</sup>. **Anal. Calc.** for C<sub>47</sub>H<sub>47</sub>N<sub>2</sub>O<sub>2</sub>Ir: C, 65.33; H, 5.48; N, 3.24 %. **Found**: C, 65.29; H, 5.33; N, 3.38 %.

*Ir(L<sup>2</sup>)<sub>2</sub>(acac)* (**2**). A bright orange powder. Crystals were grown by evaporation of an acetonitrile solution. Yield: 0.57 g (60 %). **<sup>1</sup>H NMR** (700 MHz; CD<sub>2</sub>Cl<sub>2</sub>): δ<sub>H</sub> 8.43 (d,  $J^3_{\text{HH}} = 6.0$  Hz, 2H, H<sub>A</sub>), 7.90 (d,  $J^4_{\text{HH}} = 1.7$  Hz, 2H), 7.59 (dd,  $J^3_{\text{HH}} = 7.7$  Hz,  $J^4_{\text{HH}} = 1.1$  Hz, 2H, H<sub>G</sub>), 7.20 (dd,  $J^3_{\text{HH}} = 6.0$  Hz,  $J^4_{\text{HH}} = 1.7$  Hz, 2H, H<sub>B</sub>), 6.87 (td,  $J^3_{\text{HH}} = 7.7$  Hz,  $J^4_{\text{HH}} = 1.1$  Hz, 2H, H<sub>F</sub>), 6.71 (td,  $J^3_{\text{HH}} = 7.7$  Hz,  $J^4_{\text{HH}} = 1.1$  Hz, 2H, H<sub>E</sub>), 6.27 (dd,  $J^3_{\text{HH}} = 7.7$  Hz,  $J^4_{\text{HH}} = 1.1$  Hz, 2H, H<sub>D</sub>), 5.28 (s, 1H, H<sub>J</sub>), 1.80 (s, 6H, H<sub>K</sub>), 1.20 (m, 42 H, H<sub>H+I</sub>) ppm. **<sup>13</sup>C{<sup>1</sup>H} NMR** (176 MHz; CD<sub>2</sub>Cl<sub>2</sub>): δ<sub>C</sub> 184.9, 168.5, 147.8, 144.1, 133.3, 132.3, 129.5, 124.2, 124.0, 121.1, 120.8, 104.0, 101.0, 98.9, 28.9, 18.8, 11.4 ppm. **MS-MALDI**: 960.2 [M]<sup>+</sup>. **Anal. Calc.** for C<sub>49</sub>H<sub>63</sub>N<sub>2</sub>IrO<sub>2</sub>Si<sub>2</sub>: C, 61.28; H, 6.61; N, 2.92 %. **Found**: C, 61.33; H, 6.70; N, 3.04 %.

*Ir(L<sup>3</sup>)<sub>2</sub>(acac)* (**3**). A bright orange powder. Crystals were grown by the evaporation of a DCM solution. Yield: 831 mg (68 %). **<sup>1</sup>H NMR** (700 MHz; CD<sub>2</sub>Cl<sub>2</sub>): δ<sub>H</sub> 8.60 (d,  $J^3_{\text{HH}} = 6.0$  Hz, 2H, H<sub>a</sub>), 8.12 (s, 2H, H<sub>c</sub>), 7.81 (d,  $J^3_{\text{HH}} = 8.0$  Hz, 4H, H<sub>j</sub>), 7.71 (d,  $J^3_{\text{HH}} = 7.9$  Hz,  $J^4_{\text{HH}} = 1.3$  Hz, 2H, H<sub>g</sub>), 7.68 (d,  $J^3_{\text{HH}} = 8.0$  Hz, 4H, H<sub>i</sub>), 7.43 (dd,  $J^3_{\text{HH}} = 6.0$  Hz,  $J^4_{\text{HH}} = 2.1$  Hz, 2H, H<sub>b</sub>), 6.90 (td,  $J^3_{\text{HH}} = 7.4$  Hz,  $J^4_{\text{HH}} = 1.2$  Hz, 2H, H<sub>f</sub>), 6.74 (td,  $J^3_{\text{HH}} = 7.4$  Hz,  $J^4_{\text{HH}} = 1.3$  Hz, 2H, H<sub>e</sub>), 6.37 (dd,  $J^3_{\text{HH}} = 6.0$  Hz,  $J^4_{\text{HH}} = 1.2$  Hz, 2H, H<sub>d</sub>), 5.32 (s, 1H), 1.85 (s, 6H), 1.19 (pseudo singlet, 42 H) ppm. **<sup>13</sup>C{<sup>1</sup>H} NMR** (176 MHz; CD<sub>2</sub>Cl<sub>2</sub>): δ<sub>C</sub> 184.8, 168.3, 148.4, 148.2, 147.5, 144.9, 137.1, 133.2, 132.6, 128.9, 127.0,

124.8, 123.8, 120.8, 119.7, 115.9, 106.2, 100.3, 93.0, 28.3, 18.4, 11.3 ppm. **MS-MALDI:** 1112.4 [M]<sup>+</sup>. **Anal. Calc.** for C<sub>61</sub>H<sub>71</sub>N<sub>2</sub>IrO<sub>2</sub>Si<sub>2</sub>: C, 65.85; H, 6.43; N, 2.52 %. **Found:** C, 65.81; H, 6.60; N, 2.42 %.

*Ir(L<sup>4</sup>)<sub>2</sub>(acac) (4)*. A bright green powder. Crystals were grown by the slow evaporation of a benzene solution. Yield: 714 mg (57 %). <sup>1</sup>H NMR (CD<sub>2</sub>Cl<sub>2</sub>) δ: 8.55 (d,  $J^3_{\text{HH}} = 5.7$  Hz, 2H, H<sub>a</sub>), 7.84 (s, 2H, H<sub>c</sub>), 7.60 (dd,  $J^3_{\text{HH}} = 7.8$  Hz,  $J^4_{\text{HH}} = 1.3$  Hz, 2H, H<sub>g</sub>), 7.52 (s, 2H, H<sub>k</sub>), 7.48 (dd,  $J^3_{\text{HH}} = 7.7$  Hz,  $J^4_{\text{HH}} = 1.7$  Hz, 2H, H<sub>i</sub>), 7.39 (d,  $J^3_{\text{HH}} = 7.8$  Hz, 2H, H<sub>j</sub>), 7.19 (dd,  $J^3_{\text{HH}} = 5.9$  Hz,  $J^3_{\text{HH}} = 1.9$  Hz, 2H, H<sub>b</sub>), 6.87 (td,  $J^3_{\text{HH}} = 7.4$  Hz,  $J^4_{\text{HH}} = 1.3$  Hz, 2H, H<sub>f</sub>), 6.75 (td,  $J^3_{\text{HH}} = 7.4$  Hz,  $J^4_{\text{HH}} = 1.4$  Hz, 2H, H<sub>e</sub>), 6.37 (dd,  $J^3_{\text{HH}} = 7.7$  Hz,  $J^4_{\text{HH}} = 1.2$  Hz, 2H, H<sub>d</sub>), 5.35 (s, 1H, H<sub>o</sub>), 2.44 (s, 6H, H<sub>h</sub>), 1.86 (s, 6H, H<sub>n</sub>), 1.18 (pseudo singlet, 42 H, H<sub>l</sub>+H<sub>m</sub>) ppm. <sup>13</sup>C{<sup>1</sup>H} NMR (176 MHz; CD<sub>2</sub>Cl<sub>2</sub>): δ<sub>C</sub> 184.7, 167.9, 150.2, 147.6, 147.5, 145.0, 138.7, 135.6, 134.1, 133.1, 129.6, 129.3, 128.8, 128.2, 123.8, 122.4, 120.8, 118.9, 106.5, 100.4, 91.6, 28.3, 20.0, 18.4, 11.3 ppm. **MS-MALDI:** 1140.5 [M]<sup>+</sup>. **Anal. Calc.** for C<sub>63</sub>H<sub>75</sub>N<sub>2</sub>IrO<sub>2</sub>Si<sub>2</sub>: C, 66.34; H, 6.63; N, 2.46 %. **Found:** C, 66.47; H, 6.75; N, 2.59 %.

*Ir(L<sup>5</sup>)<sub>2</sub>(acac) (5)*. A bright green powder. Yield: 552 mg (41%). <sup>1</sup>H NMR (700 MHz; CD<sub>2</sub>Cl<sub>2</sub>): δ<sub>H</sub> 8.58 (d,  $J^3_{\text{HH}} = 6.0$  Hz, 2H, H<sub>a</sub>), 7.66 (s, 2H, H<sub>c</sub>), 7.54 (dd,  $J^3_{\text{HH}} = 7.8$  Hz,  $J^4_{\text{HH}} = 1.4$  Hz, 2H, H<sub>g</sub>), 7.00 (dd,  $J^3_{\text{HH}} = 5.7$  Hz,  $J^4_{\text{HH}} = 1.8$  Hz, 2H, H<sub>b</sub>), 6.86 (td,  $J^3_{\text{HH}} = 7.4$  Hz,  $J^4_{\text{HH}} = 1.3$  Hz, 2H, H<sub>f</sub>), 6.76 (td,  $J^3_{\text{HH}} = 7.4$  Hz,  $J^4_{\text{HH}} = 1.3$  Hz, 2H, H<sub>e</sub>), 6.39 (dd,  $J^3_{\text{HH}} = 7.7$  Hz,  $J^4_{\text{HH}} = 1.2$  Hz, 2H, H<sub>d</sub>), 5.37 (s, 1H, H<sub>o</sub>), 2.55-2.54 (m, 12H, H<sub>h</sub>+H<sub>i</sub>), 2.11 (s, 6H, H<sub>j</sub> or H<sub>k</sub>), 2.04 (s, 6H, H<sub>j</sub> or H<sub>k</sub>), 1.87 (s, 6H, H<sub>n</sub>), 1.20 (pseudo singlet, 42H, H<sub>l</sub>+H<sub>m</sub>) ppm. <sup>13</sup>C{<sup>1</sup>H} NMR (176 MHz; CD<sub>2</sub>Cl<sub>2</sub>): δ<sub>C</sub> 184.7, 168.2, 152.0, 148.0, 147.4, 145.2, 139.0, 136.6, 133.0, 131.1, 128.8, 123.9, 123.7, 123.0, 120.7, 119.6, 105.4, 100.4, 99.0, 28.3, 18.5,

18.3, 17.7, 11.4 ppm. **MS-MALDI:** m/z 1224.5 [M]<sup>+</sup>. **Anal. Calc.** for C<sub>69</sub>H<sub>87</sub>N<sub>2</sub>O<sub>2</sub>Si<sub>2</sub>Ir: C, 67.66; H, 7.16; N, 2.29 %. **Found:** C, 67.49; H, 6.93; N, 2.36 %.

**Sonogashira coupling general procedure.** THF (50 mL) and Et<sub>3</sub>N (5 mL) were added to TIPS protected complex **2-5** (0.20 mmol), 4-*tert*-butyliodobenzene or 1-(*tert*-butyl)-4-((4-iodophenyl)ethynyl)benzene (0.50 mmol), Pd(PPh<sub>3</sub>)<sub>4</sub> (46 mg, 0.04 mmol) and CuI (8 mg, 0.04 mmol). The solution was degassed by three freeze-pump-thaw cycles, before tetrabutylammonium fluoride (1.0 M in THF, 0.50 mL, 0.50 mmol) was added. The solution was stirred at room temperature for 12 hours before the solvent was removed. The residue was purified by silica chromatography eluted by DCM, collecting the emissive band.

*Ir(L<sup>6</sup>)<sub>2</sub>(acac)* (**6**). An orange solid. Yield: 158 mg (87 %). **<sup>1</sup>H NMR** (700 MHz; CDCl<sub>3</sub>): δ<sub>H</sub> 8.46 (d,  $J^3_{\text{HH}} = 5.9$  Hz, 2H, H<sub>a</sub>), 7.92 (s, 2H, H<sub>c</sub>), 7.57-7.53 (m, 6H, H<sub>g</sub>+H<sub>h</sub>), 7.44 (d,  $J^3_{\text{HH}} = 8.0$  Hz, 4H, H<sub>i</sub>), 7.18 (dd,  $J^3_{\text{HH}} = 5.9$  Hz,  $J^4_{\text{HH}} = 1.9$  Hz, 2H, H<sub>b</sub>), 6.82 (td,  $J^3_{\text{HH}} = 7.8$  Hz,  $J^4_{\text{HH}} = 1.2$  Hz, 2H, H<sub>f</sub>), 6.72 (td,  $J^3_{\text{HH}} = 7.7$  Hz,  $J^4_{\text{HH}} = 1.3$  Hz, 2H, H<sub>e</sub>), 6.31 (dd,  $J^3_{\text{HH}} = 7.7$  Hz,  $J^4_{\text{HH}} = 1.2$  Hz, 2H, H<sub>d</sub>), 5.21 (s, 1H, H<sub>k</sub>), 1.79 (s, 6H, H<sub>l</sub>), 1.35 (s, 18H, H<sub>j</sub>) ppm. **<sup>13</sup>C{<sup>1</sup>H} NMR** (176 MHz; CD<sub>2</sub>Cl<sub>2</sub>): δ<sub>C</sub> 184.8, 167.9, 153.1, 147.7, 147.4, 144.4, 136.9, 133.1, 132.5, 131.7, 129.0, 127.5, 125.6, 123.9, 123.5, 120.9, 120.3, 118.7, 100.3, 96.1, 85.8, 34.8, 30.8, 28.2 ppm. **MS-MALDI:** m/z 912.4 [M]<sup>+</sup>. **Anal. Calc.** for C<sub>51</sub>H<sub>47</sub>N<sub>2</sub>IrO<sub>2</sub>·<sup>3</sup>/<sub>4</sub>CH<sub>2</sub>Cl<sub>2</sub>: C, 63.69; H, 5.01; N, 2.87 %. **Found:** C, 63.40; H, 5.38; N, 2.89 %.

*Ir(L<sup>7</sup>)<sub>2</sub>(acac)* (**7**). A red powder. Crystals were grown by the evaporation of a DCM/Hexane solution. Yield: 200 mg (90 %). **<sup>1</sup>H NMR** (700 MHz; CDCl<sub>3</sub>): δ<sub>H</sub> 8.48 (d,

$J^3_{\text{HH}} = 5.9$  Hz, 2H, H<sub>a</sub>), 7.93 (d,  $J^4_{\text{HH}} = 1.8$  Hz, 2H, H<sub>c</sub>), 7.59-7.55 (m, 10H, H<sub>g</sub>+H<sub>i</sub>+H<sub>k</sub>), 7.48 (d,  $J^3_{\text{HH}} = 8.2$  Hz, 4H, H<sub>j</sub>), 7.39 (d,  $J^3_{\text{HH}} = 8.2$  Hz, 2H, H<sub>k</sub>), 7.19 (dd,  $J^3_{\text{HH}} = 5.8$ ,  $J^4_{\text{HH}} = 1.8$  Hz, 2H, H<sub>b</sub>), 6.82 (td,  $J^3_{\text{HH}} = 7.4$ ,  $J^4_{\text{HH}} = 1.2$  Hz, 2H, H<sub>f</sub>), 6.72 (td,  $J^3_{\text{HH}} = 7.4$ ,  $J^4_{\text{HH}} = 1.2$  Hz, 2H, H<sub>e</sub>), 6.30 (dd,  $J^3_{\text{HH}} = 7.8$ ,  $J^4_{\text{HH}} = 1.1$  Hz, 2H, H<sub>d</sub>), 5.22 (s, 1H, H<sub>m</sub>), 1.80 (s, 6H, H<sub>n</sub>), 1.33 (s, 18H, H<sub>i</sub>) ppm.  **$^{13}\text{C}\{^1\text{H}\}$  NMR** (176 MHz; CDCl<sub>3</sub>):  $\delta_{\text{C}}$  184.7, 168.5, 151.9, 147.7, 143.9, 133.0, 131.9, 131.6, 131.4, 129.4, 125.4, 124.6, 123.2, 121.3, 120.9, 120.3, 119.7, 100.4, 95. **MS-MALDI**: m/z 1112.3 [M]<sup>+</sup>. **Anal. Calc.** for C<sub>67</sub>H<sub>55</sub>N<sub>2</sub>IrO<sub>2</sub>·1¼CH<sub>2</sub>Cl<sub>2</sub>: C, 67.27; H, 4.76; N, 2.30 %. **Found**: C, 67.06, H; 4.67; N, 2.31 %.

*Ir(L<sup>8</sup>)<sub>2</sub>(acac)* (**8**). An orange powder. Yield: 189 mg (89 %).  **$^1\text{H}$  NMR** (700 MHz; CD<sub>2</sub>Cl<sub>2</sub>):  $\delta_{\text{H}}$  8.57 (d,  $J^3_{\text{HH}} = 6.0$  Hz, 2H, H<sub>a</sub>), 8.13 (d  $J^4_{\text{HH}} = 2.0$  Hz, 2H, H<sub>c</sub>), 7.85 (d,  $J^3_{\text{HH}} = 8.0$  Hz, 4H, H<sub>b</sub>), 7.74 (d,  $J^3_{\text{HH}} = 8.0$  Hz, 4H, H<sub>i</sub>), 7.71 (d,  $J^3_{\text{HH}} = 8.0$  Hz, 2H, H<sub>g</sub>), 7.53 (d,  $J^3_{\text{HH}} = 8.0$  Hz, 4H, H<sub>j</sub>), 7.46-7.43 (m, 6H, H<sub>b</sub>+H<sub>k</sub>), 6.90 (td,  $J^3_{\text{HH}} = 7.1$  Hz,  $J^4_{\text{HH}} = 1.3$  Hz, 2H, H<sub>f</sub>), 6.74 (td,  $J^3_{\text{HH}} = 7.1$  Hz,  $J^4_{\text{HH}} = 1.3$  Hz, 2H, H<sub>e</sub>), 6.36 (dd,  $J^3_{\text{HH}} = 7.9$  Hz,  $J^4_{\text{HH}} = 1.2$  Hz, 2H, H<sub>d</sub>), 5.34 (s, 1H, H<sub>m</sub>), 1.85 (s, 6H, H<sub>n</sub>), 1.34 (s, 18H, H<sub>i</sub>) ppm. **MS-MALDI**: m/z 1065.1[M]<sup>+</sup>. **Anal. Calc.** for C<sub>63</sub>H<sub>54</sub>IrN<sub>2</sub>O<sub>2</sub>: C, 71.16; H, 5.12; N, 2.63 %. **Found**: C, 71.19, H, 5.18; N, 2.41 %. Unable to obtain  $^{13}\text{C}$  NMR due to low solubility.

*Ir(L<sup>9</sup>)<sub>2</sub>(acac)* (**9**). Purification achieved by washing the powder by methanol followed by DCM to give a bright orange powder. Yield: 232 mg (92 %). **MS-MALDI**: m/z 1264.4 [M]<sup>+</sup>. **Anal. Calc.** for C<sub>79</sub>H<sub>63</sub>IrN<sub>2</sub>O<sub>2</sub>·1¼CH<sub>2</sub>Cl<sub>2</sub>: C, 68.62; H, 4.74; N, 1.98 %. **Found**: C, 68.62; H, 4.41; N, 2.30 %. Unable to obtain  $^1\text{H}$  or  $^{13}\text{C}$  NMR due to low solubility.

*Ir(L<sup>10</sup>)<sub>2</sub>(acac)* (**10**). A green solid. Yield: 159 mg (73 %). **<sup>1</sup>H NMR** (700 MHz; CD<sub>2</sub>Cl<sub>2</sub>):  $\delta_{\text{H}}$  8.57 (d,  $J^3_{\text{HH}} = 6.0$  Hz, 2H, H<sub>a</sub>), 7.88 (d,  $J^4_{\text{HH}} = 1.9$  Hz, 2H, H<sub>c</sub>), 7.62 (dd,  $J^3_{\text{HH}} = 7.8$  Hz,  $J^4_{\text{HH}} = 1.3$  Hz, 2H, H<sub>g</sub>), 7.58 (s, 2H, H<sub>j</sub>), 7.54-7.52 (m, 6H, H<sub>h</sub>+H<sub>i</sub>), 7.46 (m, 6H, H<sub>j</sub>+H<sub>m</sub>), 7.22 (dd,  $J^3_{\text{HH}} = 5.8$  Hz,  $J^4_{\text{HH}} = 2.0$  Hz, 2H, H<sub>b</sub>), 6.88 (td,  $J^3_{\text{HH}} = 7.5$  Hz,  $J^4_{\text{HH}} = 1.2$  Hz, 2H, H<sub>f</sub>), 6.76 (td,  $J^3_{\text{HH}} = 7.5$  Hz,  $J^4_{\text{HH}} = 1.2$  Hz, 2H, H<sub>e</sub>), 6.38 (dd,  $J^3_{\text{HH}} = 7.7$  Hz,  $J^4_{\text{HH}} = 1.2$  Hz, 2H, H<sub>d</sub>), 5.36 (s, 1H, H<sub>o</sub>), 2.47 (s, 6H, H<sub>k</sub>), 1.88 (s, 6H, H<sub>p</sub>), 1.36 (s, 18 H, H<sub>n</sub>) ppm. **<sup>13</sup>C{<sup>1</sup>H} NMR** (176 MHz; CDCl<sub>3</sub>):  $\delta_{\text{C}}$  184.7, 167.9, 151.9, 150.2, 147.6, 147.5, 145.0, 138.4, 135.7, 133.7, 133.1, 131.2, 129.5, 129.2, 128.8, 125.4, 128.8, 122.4, 120.8, 119.9, 118.9, 100.4, 90.3, 88.1, 34.7, 30.8, 28.3, 17.4 ppm. **MS-MALDI**: m/z 1093.2 [M]<sup>+</sup>. **Anal. Calc.** for C<sub>65</sub>H<sub>49</sub>IrN<sub>2</sub>O<sub>2</sub>: C, 71.47; H, 5.44; N, 2.56 %. **Found**: C, 71.34; H, 5.59; N, 2.62 %.

*Ir(L<sup>11</sup>)<sub>2</sub>(acac)* (**11**). A green powder. Yield: 235 mg (91 %). Yield: **<sup>1</sup>H NMR** (700 MHz; CD<sub>2</sub>Cl<sub>2</sub>):  $\delta_{\text{H}}$  8.56 (d,  $J^3_{\text{HH}} = 6.2$  Hz, 2H, H<sub>a</sub>), 7.87 (d,  $J^4_{\text{HH}} = 1.8$  Hz, 2H, H<sub>c</sub>), 7.62-7.54 (m, 14 H, H<sub>g</sub>+H<sub>h</sub>+H<sub>j</sub>+H<sub>i</sub>+H<sub>m</sub>), 7.50 (d,  $J^3_{\text{HH}} = 6.2$  Hz, 4H, H<sub>n</sub>), 7.44 (d,  $J^3_{\text{HH}} = 7.7$  Hz, 2H, H<sub>i</sub>), 7.42 (d,  $J^3_{\text{HH}} = 8.2$  Hz, 4H, H<sub>o</sub>), 7.22 (dd,  $J^3_{\text{HH}} = 5.8$  Hz,  $J^4_{\text{HH}} = 2.0$  Hz, 2H, H<sub>b</sub>), 6.88 (td,  $J^3_{\text{HH}} = 7.8$  Hz,  $J^4_{\text{HH}} = 1.3$  Hz, 2H, H<sub>f</sub>), 6.76 (td,  $J^3_{\text{HH}} = 7.8$  Hz,  $J^4_{\text{HH}} = 1.3$  Hz, 2H, H<sub>e</sub>), 6.37 (dd,  $J^3_{\text{HH}} = 7.7$  Hz,  $J^4_{\text{HH}} = 1.2$  Hz, 2H, H<sub>d</sub>), 5.36 (s, 1H, H<sub>q</sub>), 2.47 (s, 6H, H<sub>k</sub>), 1.87 (s, 6H, H<sub>r</sub>), 1.33 (s, 18H, H<sub>p</sub>) ppm. **MS-MALDI**: m/z 1292.4 [M]<sup>+</sup>. **Anal. Calc.** for C<sub>81</sub>H<sub>67</sub>IrN<sub>2</sub>O<sub>2</sub>·CH<sub>2</sub>Cl<sub>2</sub>: C, 71.49; H, 5.05; N, 2.03 %. **Found**: C, 71.51; H, 4.88; N, 2.05 %.

*Ir(L<sup>12</sup>)<sub>2</sub>(acac)* (**12**). A green powder. Crystals were grown by the evaporation of a DCM/MeOH solution. Yield: 183 mg (78 %). **<sup>1</sup>H NMR** (700 MHz; CD<sub>2</sub>Cl<sub>2</sub>):  $\delta_{\text{H}}$  8.59 (d,  $J^3_{\text{HH}} = 5.7$  Hz, 2H, H<sub>a</sub>), 7.69 (d,  $J^4_{\text{HH}} = 1.8$  Hz, 2H, H<sub>c</sub>), 7.57 – 7.54 (m, 6H, H<sub>g</sub>+H<sub>i</sub>), 7.44 (d,  $J^3_{\text{HH}} = 7.9$  Hz, 4H, H<sub>m</sub>), 7.03 (dd,  $J^3_{\text{HH}} = 5.7$  Hz,  $J^4_{\text{HH}} = 1.8$  Hz, 2H, H<sub>b</sub>), 6.86 (td,  $J^3_{\text{HH}} = 7.4$  Hz,  $J^4_{\text{HH}} = 1.2$  Hz, 2H, H<sub>f</sub>), 6.76 (td,  $J^3_{\text{HH}} = 7.4$  Hz,  $J^4_{\text{HH}} = 1.2$  Hz, 2H, H<sub>e</sub>), 6.40 (dd,  $J^3_{\text{HH}} =$

7.7 Hz,  $J^4_{\text{HH}} = 1.2$  Hz, 2H, H<sub>d</sub>), 5.37 (s, 1H, H<sub>o</sub>), 2.60-2.58 (m, 12H, H<sub>i</sub>+H<sub>k</sub>), 2.14 (s, 6H, H<sub>h</sub> or H<sub>j</sub>), 2.07 (s, 6H, H<sub>h</sub> or H<sub>j</sub>), 1.88 (s, 6H, H<sub>p</sub>), 1.36 (s, 18H, H<sub>n</sub>) ppm.  $^{13}\text{C}\{^1\text{H}\}$  NMR (176 MHz; CDCl<sub>3</sub>):  $\delta_{\text{C}}$  184.7, 168.2, 152.0, 151.6, 148.0, 147.4, 145.2, 138.9, 136.2, 136.1, 133.0, 131.2, 131.1, 130.9, 128.8, 125.4, 123.9, 123.5, 123.0, 120.7, 120.6, 119.6, 100.4, 97.5, 87.5, 34.6, 30.8, 28.3, 18.2, 17.7 ppm. **MS-ASAP:** m/z 1176.515 [M]<sup>+</sup>. **Anal. Calc.** for C<sub>71</sub>H<sub>71</sub>N<sub>2</sub>O<sub>2</sub>Ir: C, 72.48; H, 6.08; N, 2.38 %. **Found:** C, 72.62; H, 5.93; N, 1.92 %.

*Ir(L<sup>13</sup>)<sub>2</sub>(acac)* (**13**). A green powder. Crystals were grown by the evaporation of a DCM/MeOH solution. Yield: 233 mg (85 %).  $^1\text{H}$  NMR (700 MHz; CD<sub>2</sub>Cl<sub>2</sub>):  $\delta_{\text{H}}$  8.60 (d,  $J^3_{\text{HH}} = 6.0$  Hz, 2H, H<sub>a</sub>), 7.70 (s, 2H, H<sub>c</sub>), 7.61-7.56 (m, 10H, H<sub>g</sub>+H<sub>i</sub>+H<sub>m</sub>), 7.50 (d,  $J^3_{\text{HH}} = 7.8$  Hz, 4H, H<sub>n</sub>), 7.42 (d,  $J^3_{\text{HH}} = 7.8$  Hz, 4H, H<sub>o</sub>), 7.04 (dd,  $J^3_{\text{HH}} = 5.7$  Hz,  $J^4_{\text{HH}} = 1.9$  Hz, 2H, H<sub>b</sub>), 6.87 (td,  $J^3_{\text{HH}} = 7.4$  Hz,  $J^4_{\text{HH}} = 1.2$  Hz, 2H, H<sub>f</sub>), 6.77 (td,  $J^3_{\text{HH}} = 7.4$  Hz,  $J^4_{\text{HH}} = 1.2$  Hz, 2H, H<sub>e</sub>), 6.41 (dd,  $J^3_{\text{HH}} = 7.8$  Hz,  $J^4_{\text{HH}} = 1.3$  Hz, 2H, H<sub>d</sub>), 5.38 (s, 1H, H<sub>q</sub>), 2.63-2.60 (m, 12 H, H<sub>i</sub>+H<sub>k</sub>), 2.14 (s, 6H, H<sub>j</sub> or H<sub>h</sub>), 2.08 (s, 6H, H<sub>j</sub> or H<sub>h</sub>), 1.88 (s, 6H, H<sub>r</sub>), 1.35 (s, 18H, H<sub>p</sub>) ppm.  $^{13}\text{C}\{^1\text{H}\}$  NMR (176 MHz; CDCl<sub>3</sub>):  $\delta_{\text{C}}$  184.8, 168.2, 152.0, 148.0, 147.4, 145.2, 139.3, 136.4, 133.0, 131.4, 131.2, 128.8, 125.4, 123.9, 123.4, 123.1, 123.0, 120.8, 119.8, 119.6, 100.4, 97.0, 91.3, 90.2, 88.3, 34.7, 30.8, 28.3, 18.3, 17.7 ppm. **MS-MALDI:** m/z 1376.4 [M]<sup>+</sup>. **Anal. Calc.** for C<sub>87</sub>H<sub>79</sub>N<sub>2</sub>O<sub>2</sub>Ir·CH<sub>2</sub>Cl<sub>2</sub>: C, 72.31; H, 5.59; N, 1.92%. **Found:** C, 72.31; H, 5.78; N, 1.92%.

## X-ray Crystallography

The X-ray single crystal data have been collected using  $\lambda\text{MoK}\alpha$  radiation ( $\lambda = 0.71073\text{\AA}$ ) on a Bruker D8Venture (Photon100 CMOS detector, I $\mu$ S-microsource, focusing mirrors) (

compounds L1HA, 1, 3, 7 and 12) Bruker SMART CCD 6000 (fine-focus sealed tube, graphite monochromator, MonoCap optics) (compounds 4 and 7) and Agilent XCalibur (Sapphire-3 CCD detector, fine-focus sealed tube, graphite monochromator) (4-(2,3,5,6-tetramethylphenyl)pyridine, 4-(2,3,5,6-tetramethyl-4-((triisopropylsilyl)ethynyl)phenyl)pyridine and L<sup>1</sup>HB) diffractometers equipped with a Cryostream (Oxford Cryosystems) open-flow nitrogen cryostats at the temperature 120.0(2)K. All structures were solved by direct method and refined by full-matrix least squares on F<sup>2</sup> for all data using Olex2<sup>14</sup> and SHELXTL<sup>15</sup> software. All non-disordered non-hydrogen atoms were refined anisotropically, hydrogen atoms in structures 4-(2,3,5,6-tetramethylphenyl)pyridine and L<sup>1</sup>HA were refined isotropically; hydrogen atoms in other structures were placed in calculated positions and refined in riding mode. The crystals 1 and 13 contain severely disordered solvent molecules (most probably DCM) that could not be modelled properly. Their contribution to the scattering was taken into account by application a MASK procedure of Olex2 program package.

Crystal data and parameters of refinement are listed in Table S1-3. Crystallographic data for the structure have been deposited with the Cambridge Crystallographic Data Centre as supplementary publication CCDC-1837878-1837887.

## **Instrumentation**

All the photophysical measurements of iridium complexes were performed using DCM as the solvent. The UV-Visible spectra were measured on a Unicam UV2-100 spectrometer operated with the Unicam Vison software in quartz cuvettes with path length  $l = 1$  cm.

Excitation and emission photoluminescence spectra were recorded on a Horiba Jobin Yvon SPEX Fluorolog 3-22 spectrofluorometer. Samples were degassed by repeated freeze-pump-thaw cycles using a turbomolecular pump until the pressure was stable in quartz cuvettes,  $l = 1$  cm. The solutions had absorbance below 0.15 to minimise inner filter effects. PLQYs were measured following the method of Resch-Genger et al.<sup>16</sup>

Emission lifetimes were recorded by exciting the sample with the output of a pulsed laser diode which produced a 1 kHz train of pulses of 20 ns duration at 405 nm. The luminescence was collected at 90° and focused onto the entrance slit of a monochromator (Betham TM-300V). The emission was detected by a photon-counting PMT and the arrival times of photons at the detector were determined using a digital oscilloscope (NI-5133) configured as a virtual multichannel by LabVIEW. The data were transferred to a PC and analysed using non-linear regression to a single exponential decay, and the quality of fit established by reduced  $\chi^2$  and random residuals. The samples were degassed by repeated freeze-pump-thaw cycles in duplicates. The decay data were fitted to exponential functions.

Electrochemical analyses of the iridium complexes were carried out using a PalmSens EmStat<sup>2</sup> potentiometer, with platinum working, platinum counter and platinum pseudo reference electrodes, from solutions in DCM containing 0.1 M supporting electrolyte (tetrabutylammonium hexafluorophosphate, TBAPF<sub>6</sub>), scan rate = 100 mV s<sup>-1</sup>. The ferrocene/ferrocinium couple was used as the internal reference.

## Computational

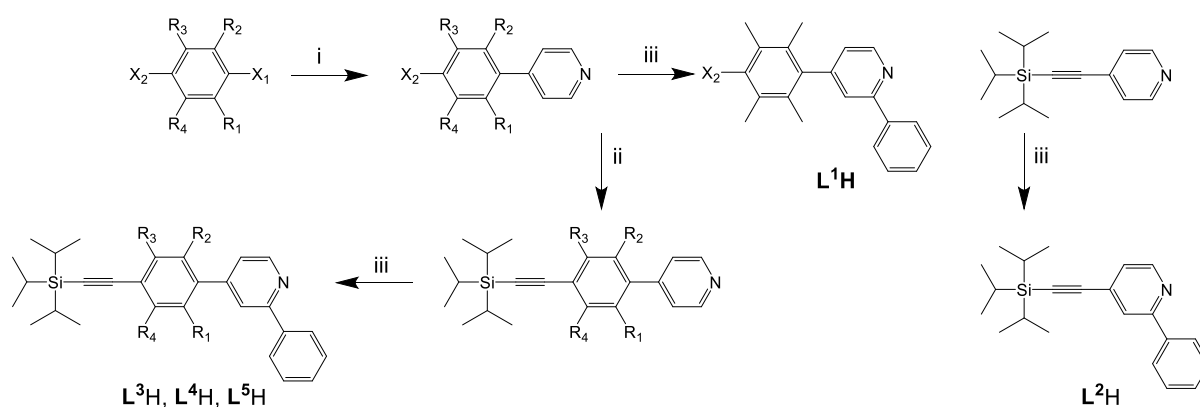
Density functional theory (DFT) calculations were carried out using the Gaussian 09 package (Gaussian, Inc)<sup>17</sup>, all results were displayed using GaussView<sup>18</sup> and GaussSum<sup>19</sup>. All calculations used the B3LYP level set employing a 6-31G(d)/LANL2DZ basis set,

geometrically optimised in a DCM solvent field using the SCRF-PCM method, with energy minima confirmed by frequency calculations.

## RESULTS AND DISCUSSION

**Synthesis.** 5 new ligands ( $L^1H$ - $L^5H$ ) were synthesized by a combination of Suzuki-Miyaura, Sonogashira couplings, and phenylation reactions.  $L^2H$  was readily synthesized by phenylation of 4-(triisopropylsilyl)ethynyl-pyridine using phenyllithium as described previously by Edkins.<sup>20</sup>  $L^{1,3-5}H$  required a Suzuki reaction with either 4-pyridylboronic acid ( $L^3H$ ), previously reported by Marks,<sup>21</sup> or 4-(4,4,5,5-tetramethyl-1,3,2-dioxaborolan-2-yl)pyridine ( $L^{1,4,5}H$ ) with bromodurene ( $L^1H$ ), 1,4-bromo-iodo-benzene ( $L^3H$ ) or 2-iodo-5-bromo-toluene ( $L^4H$ ) to give the respective 4-(4-bromophenyl)pyridine that was in turn reacted via a Sonogashira coupling to yielding the respective 4-(4-((triisopropylsilyl)ethynyl)phenyl)pyridine that was finally phenylated as with  $L^1H$ . An attempt to make 4-(4-bromo-2,6-dimethylphenyl)pyridine was made via a Suzuki between 4-(4,4,5,5-tetramethyl-1,3,2-dioxaborolan-2-yl)pyridine and 5-bromo-2-iodo-1,3-dimethylbenzene, however, due to the steric hindrance from the ortho-methyl groups the reactivity of the iodo group was reduced resulting in the production of 4-(4-iodo-3,5-dimethylphenyl)pyridine that could not be separated from the desired product. When 1-bromo-4-iodo-durene was used in place of 5-bromo-2-iodo-1,3-dimethylbenzene the selectivity of the iodo group was restored allowing for the selective synthesis of 4-(4-bromo-2,3,5,6-tetramethylphenyl)pyridine, however, the subsequent Sonogashira reaction between this and triisopropylsilyl acetylene (TIPSCCH) did not proceed, likely again due to the reduced reactivity of the bromine and increased steric hindrance. Therefore, 4-(4-iodo-2,3,5,6-tetramethylphenyl)pyridine was prepared according to Yamashita's method of

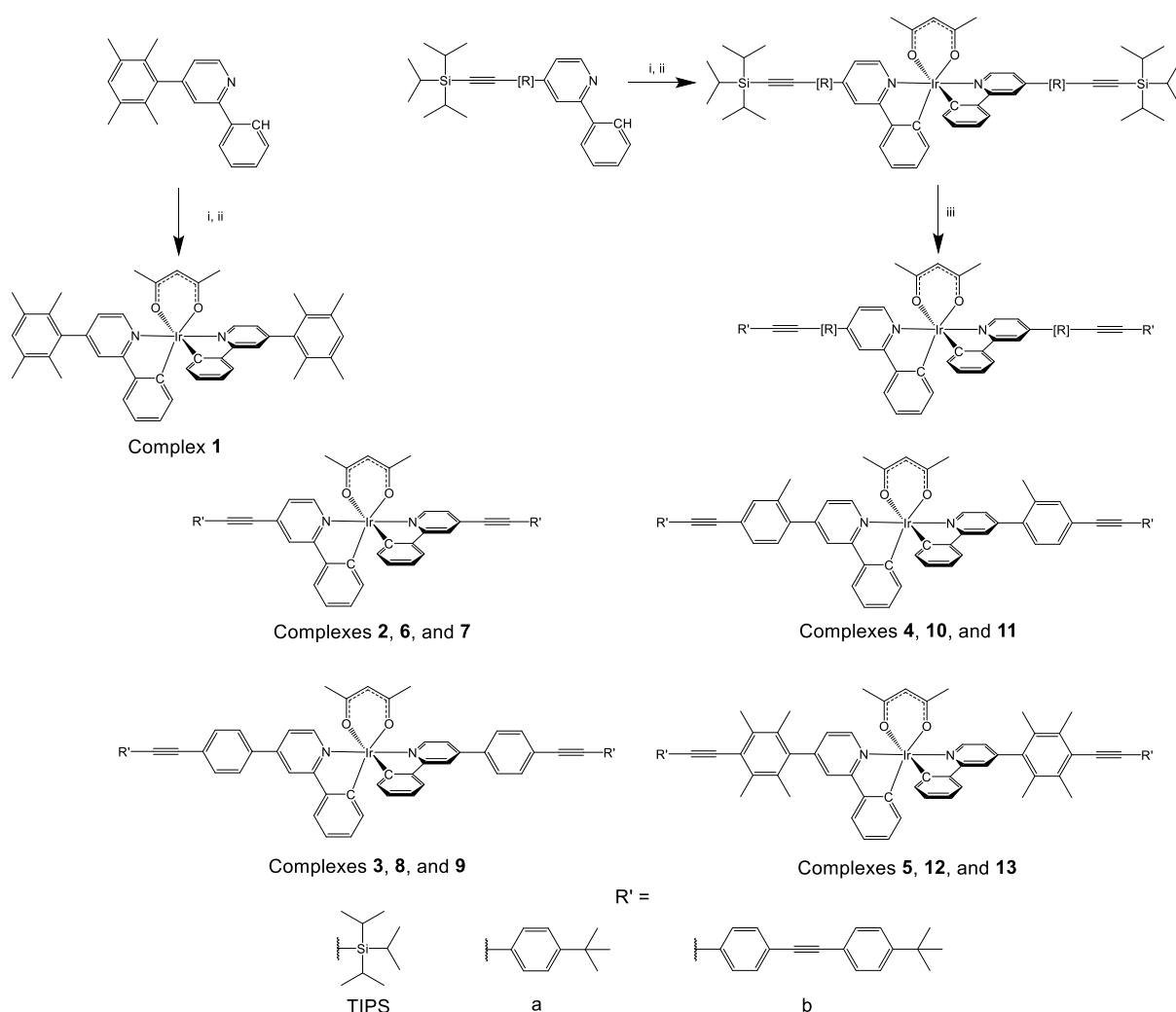
reacting 3 equivalents of diiododurene with 1 equivalent 4-(4,4,5,5-tetramethyl-1,3,2-dioxaborolan-2-yl)pyridine.<sup>22</sup> The increased reactivity of the iodo group allowed the Sonogashira reaction to proceed in reasonable yields (75%), although it was necessary to heat the reaction to 70°C to achieve this. As with the other ligands the **L**<sup>5</sup>**H** was produced by phenyllating 4-(2,3,5,6-tetramethyl-4-((triisopropylsilyl)ethynyl)phenyl)pyridine with phenyllithium.



**Scheme 1.** Schematic diagram for ligand (**L**<sup>1</sup>-**L**<sup>5</sup>**H**) synthesis where **L**<sup>1</sup>**H** ( $R_1 = R_2 = R_3 = R_4 = \text{CH}_3$ ,  $X_1 = \text{Br}$ ,  $X_2 = \text{H}$ ), **L**<sup>3</sup>**H** ( $R_1 = R_2 = R_3 = R_4 = \text{H}$ ,  $X_1 = \text{I}$ ,  $X_2 = \text{Br}$ ), **L**<sup>4</sup>**H** ( $R_1 = \text{CH}_3$ ,  $R_2 = R_3 = R_4 = \text{H}$ ,  $X_1 = \text{I}$ ,  $X_2 = \text{Br}$ ), **L**<sup>5</sup>**H** ( $R_1 = R_2 = R_3 = R_4 = \text{CH}_3$ ,  $X_1 = \text{I}$ ,  $X_2 = \text{I}$ ); i)  $\text{Pd}(\text{PPh}_3)_4$ ,  $\text{K}_2\text{CO}_3$ , 4-(4,4,5,5-tetramethyl-1,3,2-dioxaborolan-2-yl)pyridine, DMF; ii) TIPSCCH, CuI,  $\text{Pd}(\text{PPh}_3)_4$ , THF,  $^i\text{Pr}_2\text{NH}$ ; iii) PhLi, THF.

The iridium complexes **1-5** were synthesized using standard conditions, reacting the respective ligand (**L**<sup>1</sup>-**L**<sup>5</sup>**H**) with  $\text{IrCl}_3 \cdot 3\text{H}_2\text{O}$  in 2-ethoxyethanol and water to form the  $\mu$ -chloro dimer, followed by the coordination of the ancillary acac ligand using  $\text{K}_2\text{CO}_3$  and acetylacetonone. To produce the extended complexes **6-12** the complexes **2-5** were deprotected *in situ* using tetrabutylammonium fluoride (TBAF) to give the corresponding terminal alkyne making it available for Sonogashira reactions. In this case we chose to use 4-

(*tert*-butyl)iodobenzene (to give the complexes **6**, **8**, **10** and **12**) or 1-(*tert*-butyl)-4-((4-iodophenyl)ethynyl)benzene yielding complexes **7**, **9**, **11** and **13**. These groups were chosen as the increase the aspect ratio of the complexes and to attempt to enhance solubility. Despite the inclusion of a tertiary butyl group to maintain solubility complex **9** was too insoluble for even  $^1\text{H}$  NMR so could only be characterized by elemental analysis and mass-spectrometry. However, as was observed by Kozhevnikov *et al.* the inclusion of a twist in the iridium complex can greatly improve its solubility in particular complexes **10**, **11**, **12** and **13**.<sup>13</sup>



**Scheme 2.** Synthesis of complexes **1-5** and their post-synthetic modification to give complexes **6-13**. Where **2** ( $\text{R}' = \text{TIPS}$ ), **3** ( $\text{R}' = \text{TIPS}$ ), **4** ( $\text{R}' = \text{TIPS}$ ), **5** ( $\text{R}' = \text{TIPS}$ ), **6** ( $\text{R}' =$

a), **7** (R' = b), **8** (R' = a), **9** (R' = b), **10** (R' = a), **11** (R' = b), **12** (R' = a), and **13** (R' = b); i) IrCl<sub>3</sub>·3H<sub>2</sub>O, 2-ethoxyethanol and water; ii) acetylacetone, K<sub>2</sub>CO<sub>3</sub> and 2-ethoxyethanol; iii) TBAF, CuI, Pd(PPh<sub>3</sub>)<sub>4</sub>, THF, <sup>i</sup>Pr<sub>2</sub>NH and 1-(*tert*-butyl)-4-iodobenzene (**6**, **8**, **10** and **12**) or 1-(*tert*-butyl)-4-((4-iodophenyl)ethynyl)benzene (**7**, **9**, **11** and **13**).

## Molecular Structures

Crystal structures of compounds 4-(2,3,5,6-tetramethylphenyl)pyridine, 4-(2,3,5,6-tetramethyl-4-((triisopropylsilyl)ethynyl)phenyl)pyridine, **L<sup>1</sup>H** (two polymorphs) and complexes **1**, **3**, **4**, **7**, **12**, and **13** have been determined by single-crystal X-ray diffraction method. The free ligand **L<sup>1</sup>H** exists in two polymorph modifications. The conformation of molecules of two polymorphs is different: the torsion angles around the C-C bonds between pyridine ring and substituted and unsubstituted Ph-rings are 79.9(2), 32.2(2) and 88.8(4), 14.4(5)° in each of the polymorphs respectively. The packing of the molecules **L<sup>1</sup>H** in both polymorphs are determined mainly by C(Ph)-H...N interactions but packing motifs are quite different probably because in one of the polymorphs the *m*-H atom of Ph-group participate in intermolecular contacts while in the second one the corresponding *p*-H atom form the link with the adjacent Py-ring. Interestingly, no  $\pi$ ... $\pi$  interactions have been found in the discussed structures.

The crystal structure of complex **1** contains 3.5 independent molecules (one of the complexes is located in a special position on a 2-fold axis). The independent complexes **1** differ by orientation of duryl-groups, indicating conformational flexibility of the **L<sup>1</sup>H** ligand: corresponding torsion angles vary from 63.8 to 89.0°. Crystal structure of complex **3**, showing severe disorder of the terminal acetyl TIPS-groups, also contains 2 crystallographically independent molecules. The complexes **3** and DCM solvent molecules are linked by various CH...O and  $\pi$ ... $\pi$  interactions into diffuse layers, separated by the hydrophobic areas formed

out of *i*-Pr-groups. Similar packing pattern is also observed in the structure **4**, however the CH...O interactions there are replaced by CH... $\pi$  ones and the benzene solvent molecules are filling the voids. The introduction of Me-group in the side chain predictably increases torsion angle around the bond between corresponding aromatic rings from av. 27° in **3** to 40° in **4**. Complex **7** shows great conformational lability of terminal aromatic rings which form the interplanar angles with adjacent middle rings of 7.8 and 81.7°. Pyridine and duryl rings in molecule **12** in crystal form interplanar angles -77.8(7) and -65.3(7)°, the values close to those found in the complex **1**, while the terminal phenyl rings rotate relatively to the duryl ring by -37.4(6) and -11.7(6)°. Double  $\pi$ ... $\pi$  interactions link molecules **12** in crystal in centrosymmetric dimers, while various CH...O and CH... $\pi$  contacts form a further 3D-network. Quite similar molecular conformation is adopted by complex **13**. The molecule in the crystal is noticeably bent and the terminal rings are significantly differently orientated relatively to the “middle” rings of the ligand: the corresponding torsion angles are -47.0(7) and -18.4(9)°, indicating unrestricted mutual rotation of these aromatic fragments. Interestingly, there are no short distinctive direction-specific intermolecular contacts in structure **13**, the complexes and DCM solvent molecules are loosely linked by weak CH... $\pi$  and CH...O interactions. Indeed, the density of crystal packing of complex **13** is just 57.8% (the corresponding values for structures **3**, **4**, **7** and **12** are 69.3, 65.0, 62.4 and 62.8%). Thus the molecular structures of the structurally studied complexes indicate low rotation barrier of unsubstituted aromatic rings around the ethynyl links.

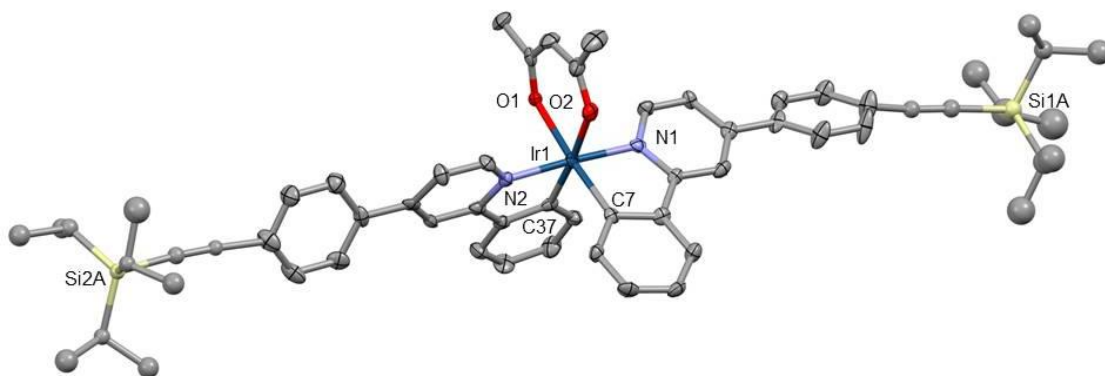


**Figure 1.** Crystal structure of **3**, solvent molecule and disorder removed for clarity, thermal ellipsoids displayed at 50% probability.

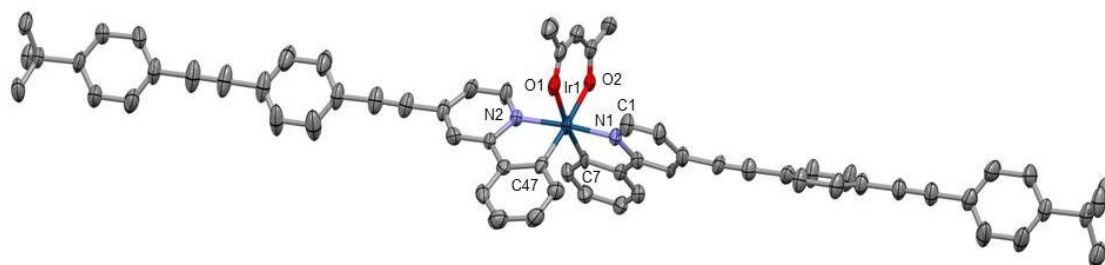


**Figure 2.** Crystal structure of **7**, solvent molecule removed for clarity, thermal ellipsoids displayed at 50% probability.

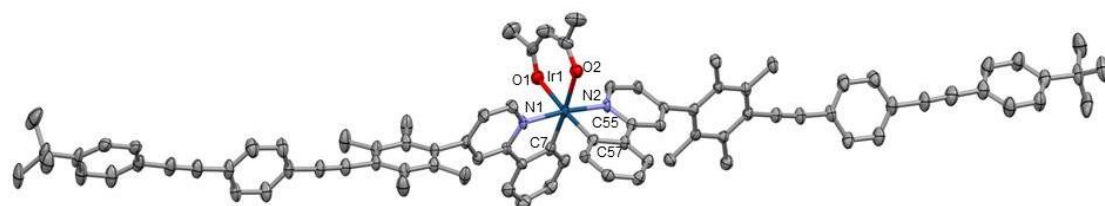


**Figure 3.** Crystal structure of **13**, solvent molecule and disorder removed for clarity, thermal ellipsoids displayed at 50% probability.

## Computational

A brief investigation was performed using DFT calculations to study the electronic structure of **1-13** and iridium(III)bis(2,4-diphenylpyridine)(acetylacetonate) ( $\text{Ir}(\text{Phppy})_2(\text{acac})$ ).

Initial geometries for complexes were based on the crystallographic structures of **1-5**, **7**, **12** and **13**. As is typical for iridium(III)(bis(2-phenylpyridine))-type complexes the HOMO is dominated by iridium and phenylate (ppy) character, with no effects occurring as a result of modification about the pyridine. Calculated HOMO energies remain in the range -5.07 – -5.17 eV. The LUMO for each of the complexes is significantly dependent on the modifications made about the pyridine. For each of the complexes **2-4** and **6-10** as the substituent attached was increased in length the LUMO energy was lowered and the relative contribution from the substituents increased, e.g. **2** (-1.94 eV, 66% Py, 21% R), **6** (-2.02 eV, 54 % Py, 36 % R) and **7** (-2.26 eV, 37 % Py, 57 % R). This occurs for each of the compounds with -, -C<sub>6</sub>H<sub>4</sub>- and -*o*tol- barrier, indicating that there is conjugation between these peripheral groups and the pyridine ring. However, when durene was used, complexes **1**, **5**, and **12** the R group was electronically decoupled, as a result the LUMO energy remained -1.44(**1**) – -1.48 (**5**) eV for all the variations and the orbital remains 64 – 65 % Py and 28 – 29 % Ph in character more characteristic of the unsubstituted Ir(ppy)<sub>2</sub>(acac). The behavior changes abruptly for **13**, with the further extension of the substituent results in a lowering of the R groups orbital energy to the point that both the LUMO and LUMO+1 are 99% substituent in character and remaining electronically decoupled from the Ir(ppy)<sub>2</sub>(acac) center of the complex.

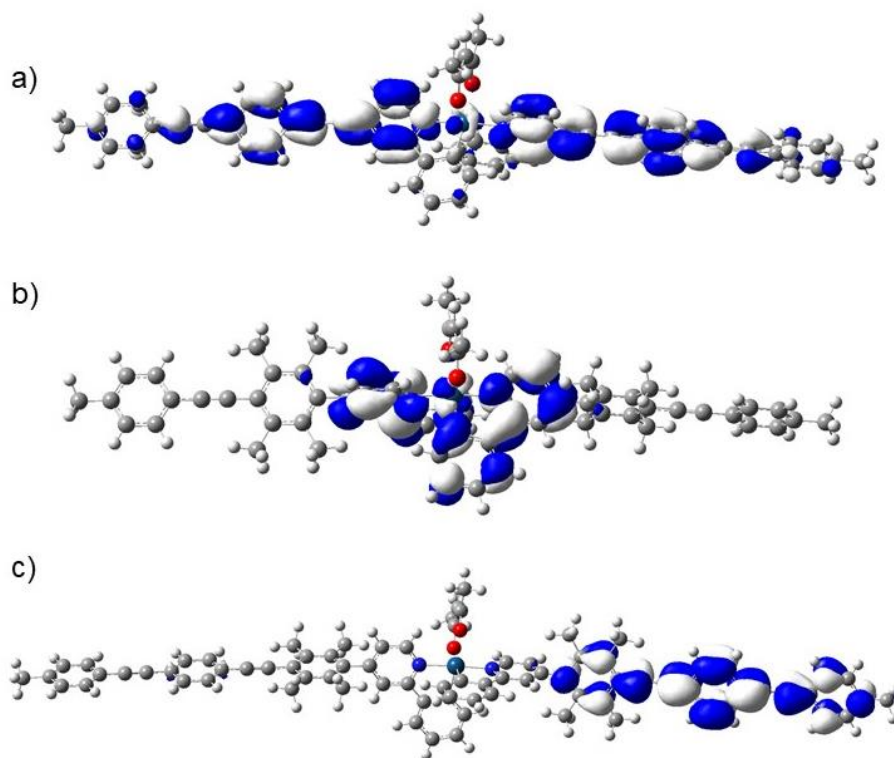


**Figure 4.** LUMO orbital diagram: a) complex **7**, b) complex **12**, c) complex **13**.

## Electrochemistry

Cyclic voltammograms were recorded for all of the complexes in 0.1 M TBAPF<sub>6</sub> in dichloromethane, and referenced against ferrocene (i.e.  $E_{1/2} \text{FeCp}_2 / [\text{FeCp}_2]^+ = 0.00 \text{ V}$ ). Each of the iridium complexes (**1-13**) show a single oxidation attributed primarily attributed to the Ir(III)/Ir(IV) couple. No reduction waves were observed within the solvent working range. The oxidation potential of the metal only ranges from 0.33 V (**1**) to 0.35 V (**3**) for all the complexes **1**, **3-5** and **8-13** and is effectively independent of the extended conjugation in the complex. However, the complexes without an aromatic spacer (**2**, **6** and **7**) have slightly higher oxidation potentials 0.36-0.38 V, this may be the result of the increased conjugation of the alkyne compared that of the aromatic groups but does not increase significantly as a result of replacing a TIPS group with a 1-(*tert*-butyl)-4-(phenylethynyl)benzene supporting that the

oxidation was localized to the Ir(ppy)<sub>2</sub>(acac) center and the alkyne is acting as an electron withdrawing group.

## Photophysical Properties

Each of the complexes **1–13** were shown to have a strong single emission ranging from 520–611 nm. In each case, the emission profile was broad and featureless, consistent with the emission being predominantly <sup>3</sup>MLCT in nature, consistent with the  $\tau_0$  values of 1.25–3.29  $\mu$ s for all complexes except **13**. The complexes with the alkyne directly attached to the pyridine (**2**, **6**, and **7**) showed a progressive red-shift as the molecules increased in length, as per Ir(ppy)<sub>2</sub>(acac) ( $\lambda_{\text{emis}} = 520$  nm, end-to-end length = 9.53 Å):<sup>23</sup> complex **2** ( $\lambda_{\text{emis}} = 582$  nm, end-to-end length = 18.79 Å); complex **6** ( $\lambda_{\text{emis}} = 585$  nm, end-to-end length = 26.21 Å); and complex **7** ( $\lambda_{\text{emis}} = 611$  nm, end-to-end length = 39.93 Å). This result is consistent with the extended conjugation of the molecule, which results in a lowering of the lowest unoccupied molecular orbital (LUMO) energy.

Furthermore, as the molecules become longer, the number of accessible vibrational modes increased along with  $k_{\text{nr}}$ , resulting in both their  $\Phi_{\text{PL}}$  and lifetimes,  $\tau_{\text{p}}$ , decreasing. The phenyl (complexes **3**, **8**, and **9**) and *o*-tolyl (complexes **4**, **10**, and **11**) groups both showed less significant red shifts with increased molecular length than complexes without the spacer, and relative to the parent molecule, e.g. phenyl Ir(Phppy)<sub>2</sub>(acac)  $\lambda_{\text{emis}} = 560$  nm:<sup>23</sup> complex **9** ( $\lambda_{\text{emis}} = 603$  nm); *o*-tolyl Ir(*o*tolppy)<sub>2</sub>(acac) ( $\lambda_{\text{emis}} = 547$  nm);<sup>24</sup> and complex **11** ( $\lambda_{\text{emis}} = 574$  nm). However, complexes with a duryl spacer showed negligible change, i.e. complex **1** ( $\lambda_{\text{emis}} = 520$  nm), and complex **13** ( $\lambda_{\text{emis}} = 524$  nm), attributed to the rotational restriction of the spacer. As the rotation becomes progressively hindered, the torsional angle between the ppy

ligand and the aromatic spacer increases (dur>*o*-tol>Ph), and the conjugation between the ppy ligand and the substituents decreases.

In poly(butyl-co-isobutyl methacrylate) (PBiBM) films, the emissions showed a small blue-shift relative to those recorded in dichloromethane (DCM) solutions e.g. **6** ( $\lambda_{\text{emis}}(\text{film}) = 553$  nm) and **7** ( $\lambda_{\text{emis}}(\text{film}) = 557$  nm) giving a  $\Delta E = 0.016$  eV compared to a  $\Delta E = 0.090$  eV in solution. This occurs for two reasons: i) the  $^3\text{MLCT}$  emission character is solvatochromic,<sup>12</sup> and ii) the increased rigidification of the polymer significantly reduces the rotational freedom of the alkynes, and as a result, hinders charge transfer.

Complexes **7** ( $\phi_{\text{PL}} = 0.38$ ) and **9** ( $\phi_{\text{PL}} = 0.28$ ) showed a lower  $\phi_{\text{PL}}$  compared to that of their shorter analogues, complexes **6** ( $\phi_{\text{PL}} = 0.54$ ) and **8** ( $\phi_{\text{PL}} = 0.54$ ). This is attributed to the increased modes of rotation resulting from the extended substituents acting as free rotors about the alkyne bonds increasing the non-radiative decay (complex **7**,  $k_{\text{nr}} = 8.99 \times 10^5 \text{ s}^{-1}$ ; complex **9**,  $k_{\text{nr}} = 7.83 \times 10^5 \text{ s}^{-1}$ ). For complexes **10–13**, the substituents sufficiently decoupled from the excited state of the complex to negate such energy losses. The TIPS-protected complexes (**2**, **3**, **4**, and **5**) had  $\phi_{\text{PL}}$  values of *ca.*, 0.20 higher than the ethynyl-phenylene substituted complexes; this result may be due to the TIPS groups protecting the phosphor center from solvent collisions.

The pure radiative emission lifetimes,  $\tau_0$ , for all of the iridium complexes (**1–12**) were 1.5–3.3  $\mu\text{s}$ , typical of iridium( $\text{C}^{\wedge}\text{N}$ )<sub>2</sub>(acac) systems. However, complex **13** had a longer lifetime of 27.5  $\mu\text{s}$  in solution but reduced to 2.23  $\mu\text{s}$  in a PBiBM film, indicative of a system exhibiting either LC type emission or reversible electronic energy transfer (REET),<sup>25–28</sup> In the latter a section of the molecule acts as a triplet sensitizer that is tethered but only weakly coupled to a phosphorescent emitter, and that the two components have triplet states that are thermally accessible to one another. The substituent of complex **13** ( $E_{\text{T1}} = 2.53$  eV, see Table 1), which

is electronically decoupled from the pyridine ring of the complex is effectively 4-((4-((4-(tert-butyl)phenyl)ethynyl)phenyl)ethynyl)-1,2,4,5-tetramethylbenzene. Compounds of this type typically have a large singlet–triplet energy gap e.g. 1,4-bis(phenylethynyl)benzene ( $E_{T1} = 2.56$  eV, see supporting information). As a result, upon excitation of the metal complex intramolecular triplet-triplet energy transfer to and from the weakly coupled 4-((4-((4-(tert-butyl)phenyl)ethynyl)phenyl)ethynyl)-1,2,4,5-tetramethylbenzene can occur which results in REET.<sup>25</sup>

**Table 1.** Electrochemical data, emission wavelengths, photoluminescence quantum yields (PLQYs), and lifetimes for iridium complexes.

	Absorption, nm ( $\epsilon$ , $\times 10^3$ L mol <sup>-1</sup> cm <sup>-1</sup> ) <sup>a</sup>	Emission (nm)		PLQY ( $\Phi$ ) <sup>a</sup>	Lifetime ( $\tau$ ), $\mu$ s		$k_r$ <sup>a</sup> $\times 10^5$ s <sup>-1</sup>	$k_{nr}$ <sup>a</sup> $\times 10^5$ s <sup>-1</sup>	Pure radiative lifetime ( $\tau_0$ ) <sup>a</sup> , $\mu$ s	$T_1$ <sup>a</sup> (eV)	$E_{ox}$ <sup>a</sup> $V_{Fc/Fc^+}$
		solution <sup>a</sup>	film <sup>b</sup>		solution <sup>a</sup>	film <sup>b</sup>					
<b>Ir(ppy)<sub>2</sub>(acac)</b> <sup>29</sup>		520	531	0.71	1.90	2.21	3.73	1.52	2.67	2.55	0.33
<b>Ir(Phppy)<sub>2</sub>(acac)</b> <sup>23</sup>		560	521	0.96	1.20	1.16	8.00	0.33	1.25	2.34	0.34
<b>Ir(otolppy)<sub>2</sub>(acac)</b> <sup>24</sup>	261(6.78), 348(1.80), 411(br), 463(br)	547	522	0.52	0.93	1.76	5.59	5.16	1.79	2.51	0.34
<b>1</b>	262(5.35), 345(1.73), 410(0.87)	520	518	0.60	1.20	2.62	5.00	3.33	2.00	2.55	0.33
<b>2</b>	265(7.43), 363(2.21), 412 (br)	586		0.65	1.20		5.42	2.92	1.85	2.36	0.38
<b>3</b>	303(10.7), 362(3.96), 470(br)	597		0.57	1.00		5.70	4.30	1.75	2.35	0.34
<b>4</b>	283(8.98), 350(2.76), 470(br)	546		0.62	0.94		6.60	4.04	1.52	2.46	0.35
<b>5</b>	261(9.27), 343(1.97), 413 (br), 465 (br), 487 (br)	521		0.66	1.01		6.53	3.37	1.53	2.53	0.35
<b>6</b>	263(5.82), 315(7.27), 366(3.74)	585	553	0.54	0.98	1.21	5.51	4.69	1.81	2.33	0.36
<b>7</b>	296(9.05), 315(10.5), 333(8.65), 371(6.59), 376(6.38)	611	557	0.38	0.69	1.41	5.51	8.99	1.82	2.27	0.38
<b>8</b>	263(5.82), 315(7.27), 366(3.74)	585	559	0.54	0.98	1.22	5.51	4.69	1.81	2.33	0.33
<b>9</b>	270(5.91), 333(9.74)	603	c	0.28	0.92	c	3.04	7.83	3.29	2.31	0.33
<b>10</b>	311(9.17), 352(3.91)	558	536	0.57	0.88	1.37	6.48	4.89	1.54	2.45	0.34
<b>11</b>	331(16.1), 470(br)	574	543	0.50	1.35	1.17	3.70	3.70	2.70	2.45	0.35
<b>12</b>	296(10.7), 313(9.13)	526	527	0.49	0.98	1.01	5.00	5.20	2.00	2.54	0.35
<b>13</b>	333(16.9), 354(14.4)	524	535	0.49	13.5	2.23	0.36	0.38	27.5	2.53	0.35

The radiative  $k_r$  and non-radiative  $k_{nr}$  values in were calculated according to the equations:

$k_r = \Phi/\tau$  and  $k_{nr} = (1 - \Phi)/\tau$ , from the quantum yields  $\Phi$  and the lifetime  $\tau$  values. <sup>a</sup>Recorded in DCM, recorded a in poly(butyl-co-isobutylmethacrylate) containing 0.1% wt film, <sup>c</sup> too insoluble to produce a homogenous film.

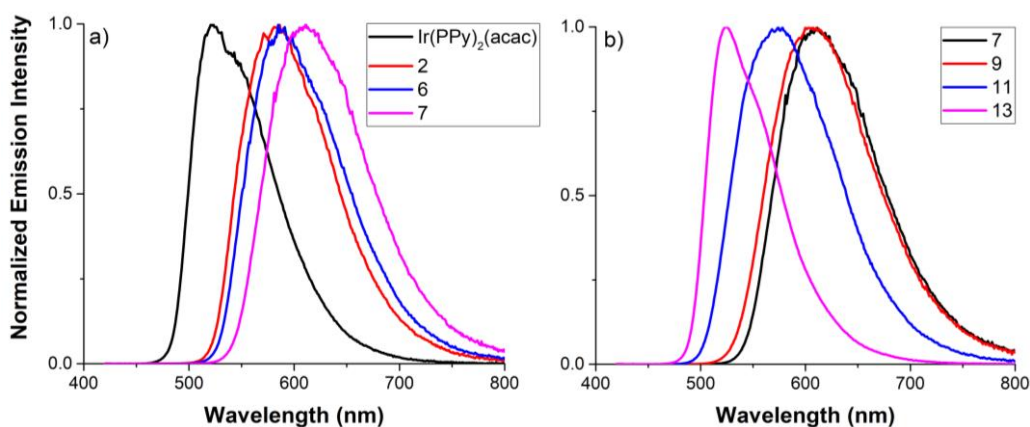


**Figure 5.** Emission spectra of iridium complexes recorded in dichloromethane (DCM),  $\lambda_{\text{ex}} = 410$  nm: a) Ir(ppy)<sub>2</sub>(acac), complexes **2**, **6**, and **7**; and b) complexes **7**, **9**, **11**, and **13**.

## OLED device fabrication and results

OLED devices incorporating complexes Ir(Phppy)<sub>2</sub>(acac), Ir(otolppy)<sub>2</sub>(acac), **1**, **6–8** and **10–13** were fabricated, with the iridium complexes blended with poly(vinyl carbazole) (PVK) as a host material and 2-(4-*tert*-butylphenyl)-5-(4-biphenyl)-1,3,4-oxadiazole (PBD) as an electron transport material to form a single, solution-processable (SP) emissive layer. Complex **9** was not included as it was too insoluble for testing in SP devices, while the TIPS intermediate complexes **2–5** were not included. As an initial characterization of these complexes, in these simple SP devices the orientations of the emitting molecules were not aligned, and therefore the polarization characteristics of the electroluminescence emission were not investigated.

Devices were fabricated in a nitrogen glove box environment on glass substrates coated with a 150 nm pre-patterned layer of indium tin oxide (ITO). A 50 nm film of poly(3,4-ethylenedioxythiophene) based dispersion (PEDOT, Clevios HIL 1.3) was deposited by spin coating, followed by spin coating of the 70 nm emissive layer from chlorobenzene solution

blended in the ratio 100:40:8 PVK:PBD:Ir by weight. A 25 nm electron transporting layer of 2,2',2''-(1,3,5-benzinetriyl)-tris(1-phenyl-1-*H*-benzimidazole) (TPBI) and LiF/Al cathode were subsequently deposited by thermal evaporation. The overall structure of the OLED devices was ITO / PEDOT (50 nm) / PVK:PBD:Ir [100:40:8] (70 nm) / TPBI (25 nm) / LiF (1 nm) / Al (100 nm).

Normalised electroluminescence emission spectra of these OLED devices are shown in Figure 6.

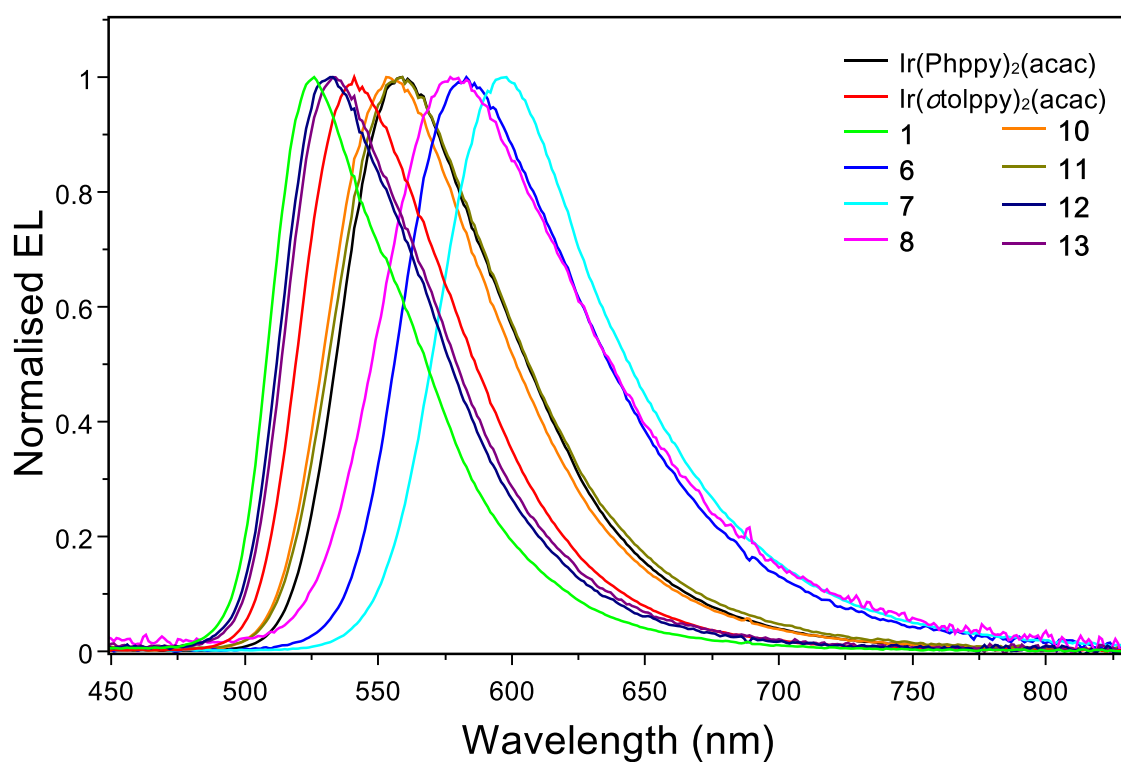


**Figure 6.** Normalised electroluminescence emission of OLED devices incorporating Ir(Phppy)<sub>2</sub>(acac), Ir(otolppy)<sub>2</sub>(acac), **1**, **6–8** and **10–13**.

The electroluminescent device emission spectra are similar to the photoluminescence emission for all complexes tested. As with the photoluminescence spectra, a red shift in

electroluminescence is observed as the length of the emitter molecules increases. For example, the maximum emission wavelength of complexes with a *o*-tolyl spacer was redshifted from 541 nm for Ir(*o*tolppy)<sub>2</sub>(acac) to 559 nm for complex **11**, while complexes with a duryl spacer showed a smaller redshift in emission from 526 nm for complex **1** to 533 nm for complex **13**. Efficiency and luminance data for all OLED devices fabricated are summarized in Table 2, and full *J-V-L* and efficiency data are shown in Figure 7.

**Table 2.** Summary of OLED device efficiency and luminance data.

Complex	$\lambda_{EL,max}$ (nm)	Maximum luminance (cd/m <sup>2</sup> )	EQE (%)	Device efficiency (cd/A)	Luminous efficacy (lm/W)	At 100 cd/m <sup>2</sup>		At 1000 cd/m <sup>2</sup>		CIE <sub>x,y</sub>
						EQE (%)	Device efficiency (cd/A)	EQE (%)	Device efficiency (cd/A)	
Ir(Phppy) <sub>2</sub> (acac)	559	13150	4.7	14.8	7.2	6.3	22.0	7.7	(0.46, 0.54)	
Ir( <i>o</i> tolppy) <sub>2</sub> (acac)	541	11300	6.4	24.1	12.6	7.4	27.7	10.2	(0.39, 0.59)	
<b>1</b>	526	8995	6.1	24.4	12.8	6.9	26.2	10.3	(0.32, 0.64)	
<b>6</b>	583	2624	2.1	5.2	1.6	2.1	4.9	1.2	(0.55, 0.45)	
<b>7</b>	598	5025	5.3	10.7	4.2	4.7	9.3	2.7	(0.59, 0.40)	
<b>8</b>	577	1208	1.1	2.6	0.7	0.6	1.5	0.3	(0.52, 0.47)	
<b>10</b>	553	9629	5.8	18.9	9.1	6.2	21.6	7.9	(0.44, 0.55)	
<b>11</b>	559	7045	5.6	18.1	8.1	5.5	18.5	6.1	(0.45, 0.54)	
<b>12</b>	532	2957	1.7	5.9	1.9	1.6	5.9	1.5	(0.35, 0.62)	
<b>13</b>	533	2473	1.2	4.5	1.6	1.4	5.2	1.3	(0.36, 0.61)	

As well as the redshift in electroluminescence, the increased molecular length of the emitter molecules results, in general, in a decrease in the overall device efficiency and luminance, as well as an increase in the turn on voltage, Figure 7.

For devices incorporating complexes with a *o*tolyl spacer, for example, a reduction in efficiency was observed from 27.7 cd/A and 7.4% EQE (at a luminance of 1000 cd/m<sup>2</sup>) for Ir(*o*tolppy)<sub>2</sub>(acac) to 18.5 cd/A and 5.5% EQE for complex **11**. The complexes with a duryl spacer (**1**, **12**, and **13**) exhibited a greater reduction in device efficiency, from 26.2 cd/A and

6.9% EQE for complex **1** to 5.2 cd/A and 1.4% EQE for complex **13**. The exception was for the complexes with the alkyne directly attached to the pyridine, where the longer, redshifted complex **7** exhibited improved device performance, at 9.3 cd/A and 4.7% EQE, compared to complex **6** at 4.9 cd/A and 2.1% EQE.

Turn on voltages required to attain a luminance of 1 cd/m<sup>2</sup> ranged from around 4.5 V for the parent complexes Ir(*otolppy*)<sub>2</sub>(*acac*), Ir(*Phppy*)<sub>2</sub>(*acac*) and complex **1**, up to 8 V for complex **8**. The higher turn on voltages correspond to increased trapping of electrons on the dopant complexes,<sup>30, 31</sup> which may be attributed to the lower LUMO energies of the longer emitter molecules. The higher turn on voltages correspond in general to the complexes with lower LUMO energies, which may be attributed to an increase in the trapping of electrons by these complexes. With only small differences in the HOMO energies across the range of complexes, and therefore in the trapping of holes, the increase in trapping of electrons caused by the lower LUMO energy affects the balance of charge carriers in the device, reducing the current density and increasing the driving voltage.<sup>32, 33</sup> Further optimisation of the device architecture for these complexes to improve the charge balance would lead to an improvement in driving voltage and device efficiency.

These device results confirm the suitability of these linear complexes for use as dopant emitters for highly efficient solution-processable OLED devices, with the potential for alignment of the emitters in order to obtain polarized device emission.

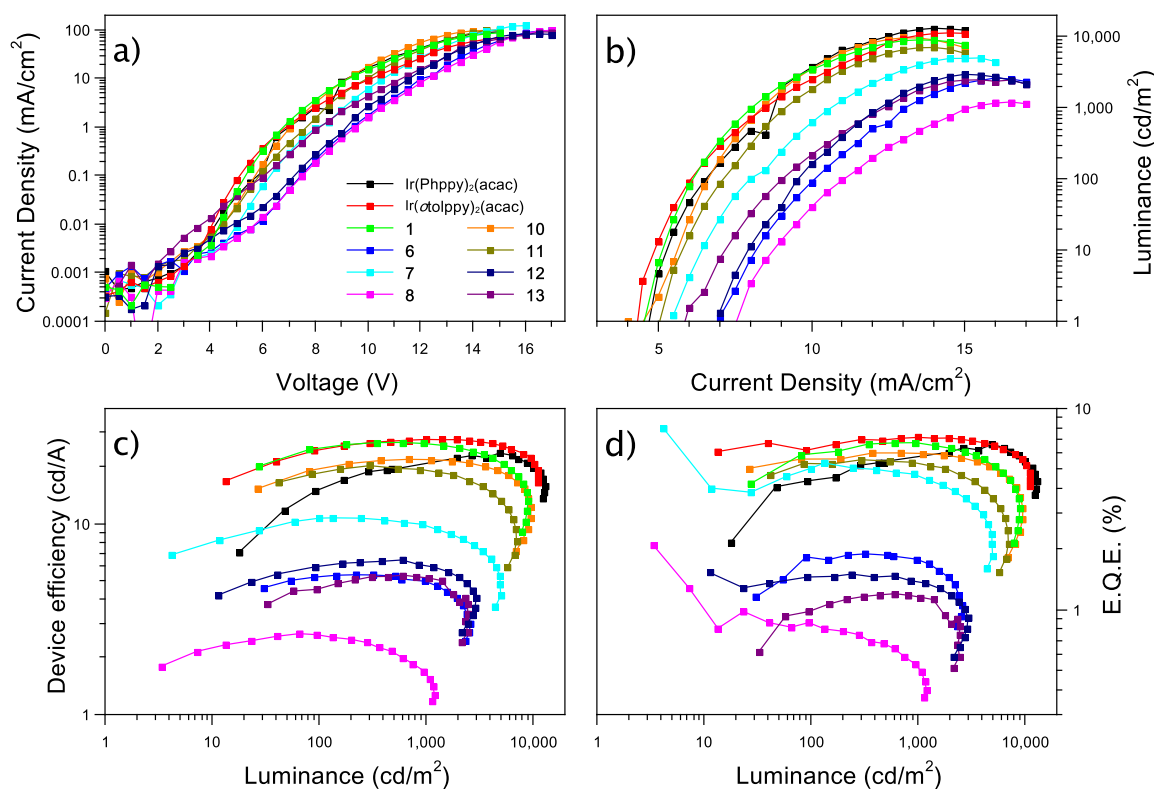


**Figure 7.** OLED efficiency and *J-V-L* data for devices incorporating Ir(Phppy)<sub>2</sub>(acac), Ir(otolppy)<sub>2</sub>(acac), **1**, **6–8** and **10–13**. Device structure ITO / PEDOT (50 nm) / PVK:PBD:Ir [100:40:8] (70 nm) / TPBI (25 nm) / LiF (1 nm) / Al (100 nm).

## Linear Alignment

As a cursory means of evaluating the effect of molecular alignment as a function of molecule length, PBiBM films containing 0.1% wt of the complexes were evaluated. The films were formed using a similar approach to that reported by Cunningham,<sup>34</sup> whereby each film was drop-cast to yield a set of approximately 1 mm thick films. These films were then heated to 60°C and stretched to twice their original length, after which they were cooled. This approach provided optically transparent films that could be stretched and that maintain elongation at room temperature. Film emission spectra were measured using a polarizing microscope (see supplementary information for details) to compare both the polarized emission spectra

parallel and perpendicular of both the original and stretched films using equation 1, where PR = polarization ratio,  $I_{\parallel}$  = the emission intensity of film parallel to the stretch direction,  $I_{\perp}$  = the emission intensity of the film perpendicular to the stretch direction, and  $f$  is the correction factor to account for the internal polarization of the optical microscope (details of determination given in supporting information).<sup>35</sup>

$$PR = \frac{I_{\parallel} - I_{\perp} f}{I_{\parallel} + I_{\perp} f} \text{ (Equation 1)}$$

Given the varied interactions of each of the complexes with the polymer, this technique reduced our ability to draw direct conclusions about individual complexes. When the polarization ratio was plotted against the end-to-end length of the all of the complexes, a general trend could be observed: each incremental increase in molecular length observed yielded a 7.1-fold increase in polarization, from Ir(ppy)<sub>2</sub>(acac) (11.6 Å) to complex **13** (49.2 Å) (Figure 8). This result indicates that an increase in the emitters' aspect ratios improves their ability to align mechanically.

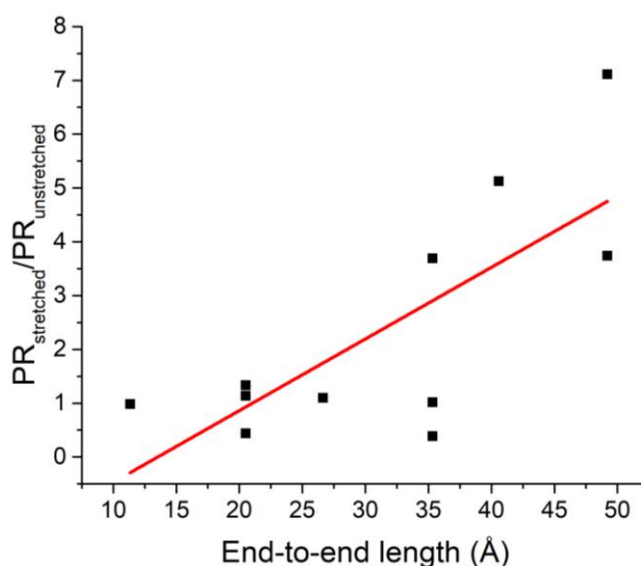


**Figure 8.** PR versus (vs.) complexes' end-to-end length for stretched poly(butyl-co-isobutyl methacrylate) PBiBM films.

## CONCLUSION

A series of iridium complexes (**1**, and **6–13**) with varied aspect ratios were synthesized through the use of TIPS-protected iridium synthons (complexes **2–5**). By de-protecting these synthons in situ, it was possible to build complexes with lengths of up to 5 nm, a length difficult to achieve by traditional means. In addition, through the incorporation of a sterically induced ‘twist’ between the Ir(ppy)<sub>2</sub>(acac) core and the substituents, it was possible to control the degree of electronic coupling between the core and the substituents, allowing for independent controls over both photophysical and mechanical behaviors. Finally, through the use of mechanical alignment of complex-containing films, it was possible to demonstrate that increases in complex length improved emission alignment in stretched polymer films.

## ASSOCIATED CONTENT

### Supporting Information.

Synthetic details for intermediate compounds (4-(2,3,5,6-tetramethylphenyl)pyridine), (4-(2,3,5,6-tetramethyl-4-((triisopropylsilyl)ethynyl)phenyl)pyridine), crystallographic data for compounds **1-4**, **6**, **7**, **12**, and **13**. NMR spectra, selected bond parameters and Cartesian coordinates for computational models are given in supporting information.

### Notes

The authors declare no competing financial interest.

## ACKNOWLEDGEMENTS

RJD gratefully acknowledge the EPSRC (EP/K007548/1) for funding this work. We would also like to thank H. D. Burrows (University of Coimbra) for the determination of the T<sub>1</sub> energy of BPEB.

## AUTHOR INFORMATION

### Corresponding Authors

\*Email: Andrew Beeby ([Andrew.Beeby@Durham.ac.uk](mailto:Andrew.Beeby@Durham.ac.uk)) and Ross Davidson  
([Ross.Davidson@Durham.ac.uk](mailto:Ross.Davidson@Durham.ac.uk))

## REFERENCES

1. Baldo, M. A.; Thompson, M. E.; Forrest, S. R. High-efficiency fluorescent organic light-emitting devices using a phosphorescent sensitizer. *Nature* **2000**, 403, 750-753.
2. Kim, K.-H.; Lee, S.; Moon, C.-K.; Kim, S.-Y.; Park, Y.-S.; Lee, J.-H.; Woo Lee, J.; Huh, J.; You, Y.; Kim, J.-J. Phosphorescent dye-based supramolecules for high-efficiency organic light-emitting diodes. *Nat. Commun.* **2014**, 5,
3. Moon, C.-K.; Kim, K.-H.; Lee, J. W.; Kim, J.-J. Influence of Host Molecules on Emitting Dipole Orientation of Phosphorescent Iridium Complexes. *Chem. Mater.* **2015**, 27, 2767-2769.
4. Zhao, L.; Komino, T.; Inoue, M.; Kim, J.-H.; Ribierre, J. C.; Adachi, C. Horizontal molecular orientation in solution-processed organic light-emitting diodes. *Appl. Phys. Lett.* **2015**, 106, 063301.
5. Mayr, C.; Taneda, M.; Adachi, C.; Brütting, W. Different orientation of the transition dipole moments of two similar Pt(II) complexes and their potential for high efficiency organic light-emitting diodes. *Org. Elec.* **2014**, 15, 3031-3037.

6. Cui, L.-S.; Liu, Y.; Liu, X.-Y.; Jiang, Z.-Q.; Liao, L.-S. Design and Synthesis of Pyrimidine-Based Iridium(III) Complexes with Horizontal Orientation for Orange and White Phosphorescent OLEDs. *ACS Appl. Mater. Interfaces* **2015**, *7*, 11007-11014.
7. Kim, K.-H.; Moon, C.-K.; Lee, J.-H.; Kim, S.-Y.; Kim, J.-J. Highly Efficient Organic Light-Emitting Diodes with Phosphorescent Emitters Having High Quantum Yield and Horizontal Orientation of Transition Dipole Moments. *Adv. Mater.* **2014**, *26*, 3844-3847.
8. Kim, S.-Y.; Jeong, W.-I.; Mayr, C.; Park, Y.-S.; Kim, K.-H.; Lee, J.-H.; Moon, C.-K.; Brütting, W.; Kim, J.-J. Organic Light-Emitting Diodes with 30% External Quantum Efficiency Based on a Horizontally Oriented Emitter. *Adv. Funct. Mater.* **2013**, *23*, 3896-3900.
9. Mayr, C.; Brütting, W. Control of Molecular Dye Orientation in Organic Luminescent Films by the Glass Transition Temperature of the Host Material. *Chem. Mater.* **2015**, *27*, 2759-2762.
10. Jurow, M. J.; Mayr, C.; Schmidt, T. D.; Lampe, T.; Djurovich, P. I.; Brütting, W.; Thompson, M. E. Understanding and predicting the orientation of heteroleptic phosphors in organic light-emitting materials. *Nat. Mater.* **2016**, *15*, 85-91.
11. Sun, P.; Li, C.; Pan, Y.; Tao, Y. Synthesis of novel Ir complexes and their application in organic light emitting diodes. *Synth. Met.* **2006**, *156*, 525-528.
12. Edkins, R. M.; Bettington, S. L.; Goeta, A. E.; Beeby, A. Two-photon spectroscopy of cyclometalated iridium complexes. *Dalton Trans.* **2011**, *40*, 12765-12770.
13. Kozhevnikov, V. N.; Zheng, Y.; Clough, M.; Al-Attar, H. A.; Griffiths, G. C.; Abdullah, K.; Raisys, S.; Jankus, V.; Bryce, M. R.; Monkman, A. P. Cyclometalated Ir(III) Complexes for High-Efficiency Solution-Processable Blue PhOLEDs. *Chem. Mater.* **2013**, *25*, 2352-2358.

14. Dolomanov, O. V.; Bourhis, L. J.; Gildea, R. J.; Howard, J. A. K.; Puschmann, H. OLEX2: a complete structure solution, refinement and analysis program. *J. Appl. Crystallogr.* **2009**, *42*, 339-341.
15. Sheldrick, G. A short history of SHELX. *Acta Crystallogr., Sect. A* **2008**, *64*, 112-122.
16. Würth, C.; Grabolle, M.; Pauli, J.; Spieles, M.; Resch-Genger, U. Relative and absolute determination of fluorescence quantum yields of transparent samples. *Nat. Protocols* **2013**, *8*, 1535-1550.
17. M. J. Frisch; G. W. Trucks; H. B. Schlegel; G. E. Scuseria; M. A. Robb; J. R. Cheeseman; G. Scalmani; V. Barone; B. Mennucci; G. A. Petersson; H. Nakatsuji; M. Caricato; X. Li; H. P. Hratchian; A. F. Izmaylov; J. Bloino; G. Zheng; J. L. Sonnenberg; M. Hada; M. Ehara; K. Toyota; R. Fukuda; J. Hasegawa; M. Ishida; T. Nakajima; Y. Honda; O. Kitao; H. Nakai; T. Vreven; J. A. Montgomery, J., J. E. Peralta, F. Ogliaro, M. Bearpark, J. J. Heyd, E. Brothers, K. N. Kudin, V. N. Staroverov, R. Kobayashi, J. Normand, K. Raghavachari, A. Rendell, J. C. Burant, S. S. Iyengar, J. Tomasi, M. Cossi, N. Rega, J. M. Millam, M. Klene, J. E. Knox, J. B. Cross, V. Bakken, C. Adamo, J. Jaramillo, R. Gomperts, R. E. Stratmann, O. Yazyev, A. J. Austin, R. Cammi, C. Pomelli, J. W. Ochterski, R. L. Martin, K. Morokuma, V. G. Zakrzewski, G. A. Voth, P. Salvador, J. J. Dannenberg, S. Dapprich, A. D. Daniels, Ö. Farkas, J. B. Foresman, J. V. Ortiz, J. Cioslowski, and D. J. Fox. *Gaussian 09*, A.1; Gaussian, Inc: Wallingford CT, 2009.
18. Dennington, R.; Keith, T.; Millam, J. *GaussView*, Version 5; Semichem Inc.: Shawnee Mission KS, 2009.
19. O'Boyle, N. M.; Tenderholt, A. L.; Langner, K. M. cclib: A library for package-independent computational chemistry algorithms. *J. Comput. Chem.* **2008**, *29*, 839-845.

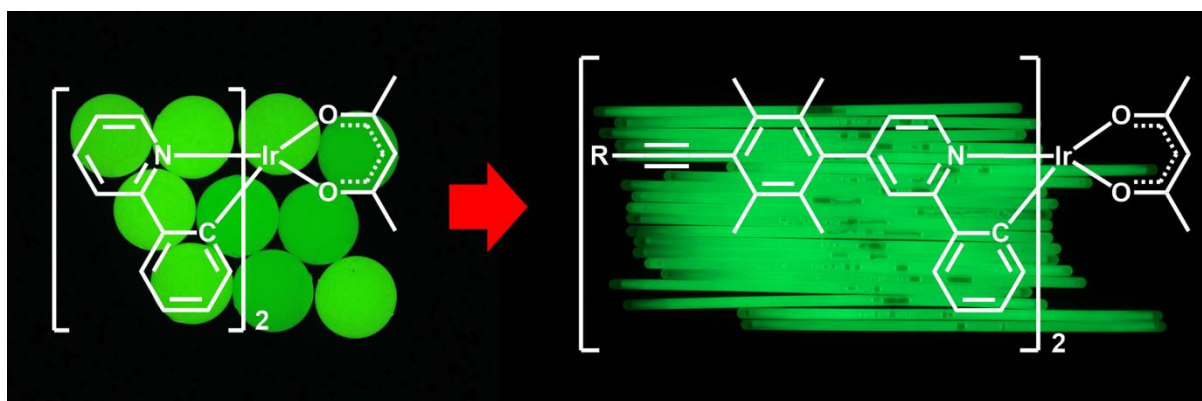
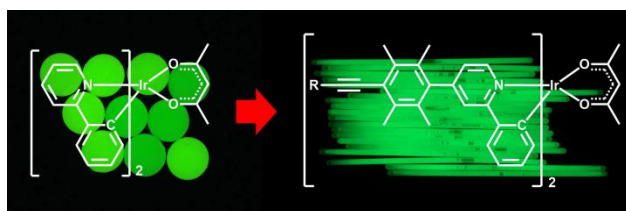
20. Edkins, R. *The Synthesis and Photophysics of Cyclometalated Iridium Complexes and Photochromic Materials*. Durham University, Durham, 2013.
21. Wang, Y.; Frattarelli, D. L.; Facchetti, A.; Cariati, E.; Tordin, E.; Ugo, R.; Zuccaccia, C.; Macchioni, A.; Wegener, S. L.; Stern, C. L.; Ratner, M. A.; Marks, T. J. Twisted  $\pi$ -Electron System Electrooptic Chromophores. Structural and Electronic Consequences of Relaxing Twist-Inducing Nonbonded Repulsions. *J. Phys. Chem. C* **2008**, 112, 8005-8015.
22. Yamashita, K.-i.; Sato, K.-i.; Kawano, M.; Fujita, M. Photo-induced self-assembly of Pt(ii)-linked rings and cages via the photolabilization of a Pt(ii)-py bond. *New J. Chem.* **2009**, 33, 264-270.
23. Edkins, R. M.; Wriglesworth, A.; Fucke, K.; Bettington, S. L.; Beeby, A. The synthesis and photophysics of tris-heteroleptic cyclometalated iridium complexes. *Dalton Trans.* **2011**, 40, 9672-9678.
24. Davidson, R.; Hsu, Y.; Batchelor, T.; Yufit, D.; Beeby, A. The use of organolithium reagents for the synthesis of 4-aryl-2-phenylpyridines and their corresponding iridium(III) complexes. *Dalton Trans.* **2016**, 45, 11496-11507.
25. Lavie-Cambot, A.; Lincheneau, C.; Cantuel, M.; Leydet, Y.; McClenaghan, N. D. Reversible electronic energy transfer: a means to govern excited-state properties of supramolecular systems. *Chem. Soc. Rev.* **2010**, 39, 506-515.
26. Denisov, S. A.; Cudré, Y.; Verwilt, P.; Jonusauskas, G.; Marín-Suárez, M.; Fernández-Sánchez, J. F.; Baranoff, E.; McClenaghan, N. D. Direct Observation of Reversible Electronic Energy Transfer Involving an Iridium Center. *Inorg. Chem.* **2014**, 53, 2677-2682.
27. Howarth, A. J.; Davies, D. L.; Lelj, F.; Wolf, M. O.; Patrick, B. O. Tuning the Emission Lifetime in Bis-cyclometalated Iridium(III) Complexes Bearing Iminopyrene Ligands. *Inorg. Chem.* **2014**, 53, 11882-11889.

28. Medina-Rodriguez, S.; Denisov, S. A.; Cudre, Y.; Male, L.; Marin-Suarez, M.; Fernandez-Gutierrez, A.; Fernandez-Sanchez, J. F.; Tron, A.; Jonusauskas, G.; McClenaghan, N. D.; Baranoff, E. High performance optical oxygen sensors based on iridium complexes exhibiting interchromophore energy shuttling. *Analyst* **2016**, 141, 3090-3097.
29. Lamansky, S.; Djurovich, P.; Murphy, D.; Abdel-Razzaq, F.; Kwong, R.; Tsyba, I.; Bortz, M.; Mui, B.; Bau, R.; Thompson, M. E. Synthesis and Characterization of Phosphorescent Cyclometalated Iridium Complexes. *Inorg. Chem.* **2001**, 40, 1704-1711.
30. Al-Attar, H. A.; Griffiths, G. C.; Moore, T. N.; Tavasli, M.; Fox, M. A.; Bryce, M. R.; Monkman, A. P. Highly Efficient, Solution-Processed, Single-Layer, Electrophosphorescent Diodes and the Effect of Molecular Dipole Moment. *Adv. Funct. Mater.* **2011**, 21, 2376-2382.
31. O'Brien, D. F.; Giebeler, C.; Fletcher, R. B.; Cadby, A. J.; Palilis, L. C.; Lidzey, D. G.; Lane, P. A.; Bradley, D. D. C.; Blau, W. Electrophosphorescence from a doped polymer light emitting diode. *Synth. Met.* **2001**, 116, 379-383.
32. Al-Attar, H. A.; Griffiths, G. C.; Moore, T. N.; Tavasli, M.; Fox, M. A.; Bryce, M. R.; Monkman, A. P. Highly Efficient, Solution-Processed, Single-Layer, Electrophosphorescent Diodes and the Effect of Molecular Dipole Moment. *Advanced Functional Materials* **2011**, 21, 2376-2382.
33. Noh, Y.-Y.; Lee, C.-L.; Kim, J.-J.; Yase, K. Energy transfer and device performance in phosphorescent dye doped polymer light emitting diodes. *The Journal of Chemical Physics* **2003**, 118, 2853-2864.
34. Cunningham, P. D.; Souza, J. B.; Fedin, I.; She, C.; Lee, B.; Talapin, D. V. Assessment of Anisotropic Semiconductor Nanorod and Nanoplatelet Heterostructures with Polarized Emission for Liquid Crystal Display Technology. *ACS Nano* **2016**, 10, 5769-5781.

35. Dekkers, J. J.; Hoornweg, G. P.; Maclean, C.; Velthorst, N. H. Fluorescence and phosphorescence polarization of molecules oriented in stretched polymers. General description. *Chemical Physics Letters* **1973**, 19, 517-523.

### TABLE OF CONTENTS/ABSTRACTS GRAPHIC

Using Sonogashira coupling with alkyne iridium(phenylpyridine)<sub>2</sub>(acetylacetonate) synthons to produce highly linearized twisted iridium(III) complexes with lengths of up to 5 nm. These complexes were mechanically aligned in a polymer matrix showing an improved contrast ratio with increased length.



---